



**IMPACTS OF RECTIFIER SELECTION ON POWER QUALITY IN A WATER
ELECTROLYSIS PLANT**

Harmonic Distortion and Reactive Power

Lappeenranta–Lahti University of Technology LUT

Master's programme in Electrical Engineering, Master's thesis

2025

Mikko Savolainen

Examiners: Professor Pasi Peltoniemi

D.Sc. (Tech.) Aleksi Mattsson

Supervisors: Senior Project Manager Mika Maranko

Electrical Operations Manager Jari Vehmaa

ABSTRACT

Lappeenranta–Lahti University of Technology LUT

LUT School of Energy Systems

Electrical Engineering

Mikko Savolainen

Impacts of Rectifier Selection on Power Quality in a Water Electrolysis Plant – Harmonic Distortion and Reactive power

Master's thesis

2025

88 pages, 33 figures, 24 tables and 5 appendices

Examiners: Professor Pasi Peltoniemi and D.Sc. (Tech.) Aleksi Mattsson

Keywords: Rectifier, power quality, power supply, harmonic distortion, reactive power, hydrogen, water electrolysis, FEL

Production of green hydrogen in water electrolysis is an interesting option for supporting the global energy transition towards the carbon neutrality goals, where the growing number of announced projects supports the insight. The water electrolysis can be stated to be an energy-intensive process, which encourages to research impacts of electrical power transmission.

Rectifiers affect power quality and control of reactive power. The rectifiers appear as non-linear load to power grid, which produces harmonic distortion. This research is processing differences between two rectifier technologies in harmonic distortion and reactive power, where total power of a 50 MW electrolysis plant at different load scenarios are simulated and impacts for power grid are evaluated.

Selected rectifier technologies are based on budgetary quotation, which is also utilized for investigate the division of CAPEX costs. Instructions for project implementation is produced, that the on-time design process can be managed and possible surprises for project costs or schedule can be minimized, considering power quality and reactive power.

Based on the simulation results, the IGBT technology doesn't require external electricity filtering or reactive power compensation, unlike the thyristor technology requires. Because of that, engineering of power distribution can be more straightforward, when utilizing the IGBT technology.

TIIVISTELMÄ

Lappeenrannan–Lahden teknillinen yliopisto LUT

LUTin energijärjestelmien tiedekunta

Sähkötekniikka

Mikko Savolainen

Tasasuuntaajavalinnan vaikutukset sähkönlaatuun vesielektrolyysilaitoksessa – Harmoniset yliaallot ja loisteho

Diplomityö

2025

88 sivua, 33 kuvaa, 24 taulukkoa ja 5 liitettä

Tarkastajat: Professori Pasi Peltoniemi ja TkT Aleks Mattsson

Avainsanat: Tasasuuntaaja, sähkönlaatu, harmoniset yliaallot, loisteho, vety, vesielektrolyysi, FEL

Vihreän vedyn tuotanto vesielektrolyysiprosessissa on mielenkiintoinen vaihtoehto tuke-
massa globaalia energiasiirtymää kohti hiilineutraalisuustavoitteita, joka voidaan päätellä
myös julkaistujen projektien kasvavasta määrästä. Vesielektrolyysiä voidaan pitää energi-
aintensiivisenä prosessina, mikä kannustaa tutkimaan sähkötehon siirtoon liittyviä vaikutuk-
sia.

Tasasuuntaajat vaikuttavat sähkönlaatuun sekä loistehon hallintaan. Tasasuuntaajat näyttä-
tyvät verkkoon päin epälineaarisenä kuormana, joka aiheuttaa harmonisia yliaalloja sähkö-
verkossa. Työssä käsitellään kahden eri tasasuuntaajateknologian välisiä eroja harmonisiin
yliaaltoihin- sekä loistehoon liittyen ja simulointien avulla paneudutaan 50 MW sähkötehoi-
sen elektrolyysilaitoksen vaikutuksiin sähköverkossa, jossa simuloidaan erilaisia kuormitus-
tilanteita.

Valitut tasasuuntaajateknologiat perustuvat budjettitarjoukseen, minkä perusteella arvioi-
daan myös teknologioiden välisiä eroja investointikustannusten jakaantumisessa. Työssä
luodaan projektiohjeistus, jonka perusteella suunnittelua voidaan ohjata oikea-aikaisesti pro-
jektin edetessä ja pyritään minimoimaan projektissa tulevia yllätyksiä sähkönlaatu ja lois-
teho huomioiden, mitkä voivat aiheuttaa haasteita projektin aikatauluun tai kustannuksiin.

IGBT-teknologia ei vaadi ulkoista sähkön suodatusta eikä loistehon kompensointia simu-
lointituloksiin perustuen, toisin kuin tyristoriteknologian todetaan vaativan. Tämän takia
IGBT-teknologian käyttö voi suoraviivaistaa sähkönjakelun suunnittelua.

ACKNOWLEDGEMENTS

This research was made possible by Helen Ltd. Implementing research without an interesting and challenging topic would be frustrating and pointless. Thank you, Helen Ltd, for the meaningful topic and special thanks for Helen's Hydrogen and power to X team for supporting during the research.

Building the simulation models were challenging, where support from LUT examiners Professor Pasi Peltoniemi and D.Sc. Alekski Mattsson was valuable.

Thank you for Helen Ltd's supervisors Senior Project Manager Mika Maranko and Electrical Operations Manager Jari Vehmaa for discussions, expertise and feedback during the research.

In Helsinki, 1.5.2025

Mikko Savolainen

SYMBOLS AND ABBREVIATIONS

Roman characters

<i>A</i>	area	cm ²
<i>C</i>	capacitance	F
<i>E</i>	energy	kWh
<i>f</i>	frequency	Hz
<i>h</i>	harmonic number	
<i>I</i>	current	A
<i>i</i>	current	A
<i>L</i>	inductance	H
<i>m</i>	modulation ratio	
<i>n</i>	number	
<i>P</i>	active power	kW, MW, GW
<i>p</i>	ratio	
<i>Q</i>	reactive power	kVAr, MVar
<i>R</i>	resistance	Ω
<i>S</i>	apparent power	MVA
<i>U</i>	source voltage	V
<i>V</i>	voltage	V
<i>X</i>	reactance	Ω
<i>Z</i>	impedance	Ω

Greek characters

α	firing angle	°
μ	commutation overlap angle	°
Φ	phase angle	°
δ	phase angle	°
ω	angular frequency	rad/s

Subscripts

0	no-load
1	primary side, fundamental
2	secondary side
3	tertiary side
a	a phase
b	base
D	DC
d	direct component
f	filter
g	grid side
h	harmonic number
IT	isolation transformer
k	short circuit value
L	maximum demand load, load
LL	line-to-line
m	magnetization

max	peak value
MOD	voltage reference
n	nominal, rated, at harmonic number
p	psophometric value
q	quadrature component
res	resonant
s	source
SC	maximum short circuit
sw	switching frequency
T	shifting
TRIANG	carrier wave
z	zero component

Abbreviations

AC	Alternating current
AEL	Alkaline
CAPEX	Capital Expenditures
CCS	Carbon Capture and Storage
DC	Direct current
DPF	Displacement power factor
e ⁻	Electron
FEED	Front-end engineering design
FEL	Front-end loading
FID	Final investment decision

GDL	Gas diffusion layer
H ⁺	Proton
HV	High voltage
IGBT	Insulated-gate bipolar transistor
LCL	LCL filter
MV	Medium voltage
OPEX	Operating Expenses
PCC	Point of common coupling
PEM	Proton Exchange Membrane
PF	Power factor
PTL	Porous transportation layer
PWM	Pulse-width modulation
Ref	Reference
SPWM	Sinusoidal pulse-width modulation
TDD	Total demand distortion
THD	Total harmonic distortion

Table of contents

Abstract

Acknowledgements

Symbols and abbreviations

1	Introduction	11
1.1	Hydrogen production and market insight	11
1.2	Green hydrogen at Helen Ltd.....	14
1.3	Role of power distribution in the production of hydrogen in water electrolysis .	14
1.4	Previous studies	15
1.5	Objectives, limitations and research questions	16
1.6	Methods and structure.....	17
2	Grid code and standards	18
2.1	Standards.....	18
2.1.1	SFS-EN 50160:2022 Voltage characteristics of electricity supplied by public electricity networks	18
2.1.2	IEEE 519-2022 Standard of harmonic control in electric power systems	19
2.2	Power quality in Fingrid's 110 kV grid	21
2.2.1	Harmonics in 110 kV power grid	21
2.3	Implementation of standards.....	23
2.4	Reactive power payments	23
3	Electrolyser parameters and selection of rectifier types.....	24
3.1	PEM water electrolysis	24
3.2	Electrolyser parameters.....	25
3.3	Selection of rectifier types	27
4	Rectifier technologies	29
4.1	Thyristor bridge rectifiers	29
4.1.1	Thyristor bridge rectifier topologies	29
4.1.2	Control and characteristics of 6-pulse thyristor bridge rectifier	30
4.1.3	Benefits of multi-pulse thyristor bridge configurations.....	34

4.2	IGBT rectifiers	36
4.2.1	PWM modulation.....	37
5	Modelling of rectifier operation	41
5.1	DC load	41
5.2	Power grid parameters	42
5.3	Main transformer parameters.....	42
5.4	Parameters for rectifier transformers	44
5.5	Thyristor rectifier model.....	46
5.5.1	Control of thyristor bridge rectifier	47
5.6	IGBT rectifier model	48
5.6.1	LCL filter	50
5.6.2	Control of the IGBT rectifier	52
5.7	Simulation results	55
5.7.1	Results of thyristor rectifier simulations.....	57
5.7.2	Results of IGBT rectifier simulations.....	65
5.8	Verification of simulation results	70
6	Distribution of CAPEX costs	72
7	Project implementation.....	74
7.1	Initial data for the project basic design work.....	76
7.2	Basic design	78
7.3	Detailed design	80
7.3.1	Power quality study	80
7.4	Verification of power quality and reactive power	81
8	Conclusions	82
8.1	Key findings.....	82
8.2	Recommendations for the future studies	84
8.3	Final words	85
	References.....	86

Appendices

Appendix 1. Psophometric weighting factors

Appendix 2. Scenario 1: Current and voltage waveforms of thyristor model

Appendix 3. Scenario 3: Current and voltage waveforms of thyristor model

Appendix 4. Scenario 1: Current and voltage waveforms of IGBT model

Appendix 5. Scenario 3: Current and voltage waveforms of IGBT model

1 Introduction

The global energy transition is needed to reduce greenhouse gas emissions and ensure energy security, where hydrogen's role is growing rapidly. Hydrogen is a clean and versatile energy carrier, which can be utilized in several industries and energy sector as well as fuel for transportation. Hydrogen can be produced from renewable energy sources which makes the hydrogen more interesting and potential energy resource. (Hassan et al. 2024)

The major industrial hydrogen consumers are refining and chemical industries as well as steel production. Transportation sector can utilize hydrogen directly for fuel cells and internal combustion engines or e-fuels manufactured from hydrogen and carbon dioxide. (Hassan et al. 2024)

1.1 Hydrogen production and market insight

Hydrogen can be divided into three categories according to the production method. The production categories are gray hydrogen, blue hydrogen and green hydrogen. Figure 1 is presenting three different categories for the hydrogen production. (Guo et al. 2023)

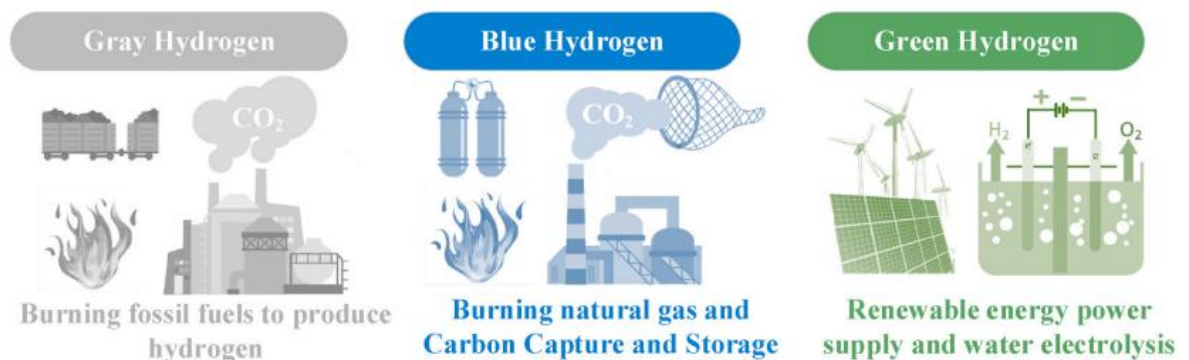


Figure 1. Different categories for hydrogen production (Guo et al. 2023).

Gray hydrogen is produced by burning fossil fuels to produce hydrogen and that don't decrease the greenhouse gas emissions. Blue hydrogen is produced for example by burning

natural gas with simultaneously using Carbon Capture and Storage (CCS), which can reduce the greenhouse gases. The least polluting is green hydrogen, which is produced in water electrolysis powered by a renewable energy source. Electricity is used to separate water to hydrogen and oxygen in the water electrolysis system. (Guo et al. 2023)

Multiple renewable hydrogen and low carbon hydrogen projects are announced worldwide which encourages for the new research related into green hydrogen production. Hydrogen insights 2024 examines global development of the hydrogen industry, where Figure 2 is presenting cumulative production capacity announced for renewable and low carbon hydrogen from year 2020 to 2030. (McKinsey & Company. 2024)

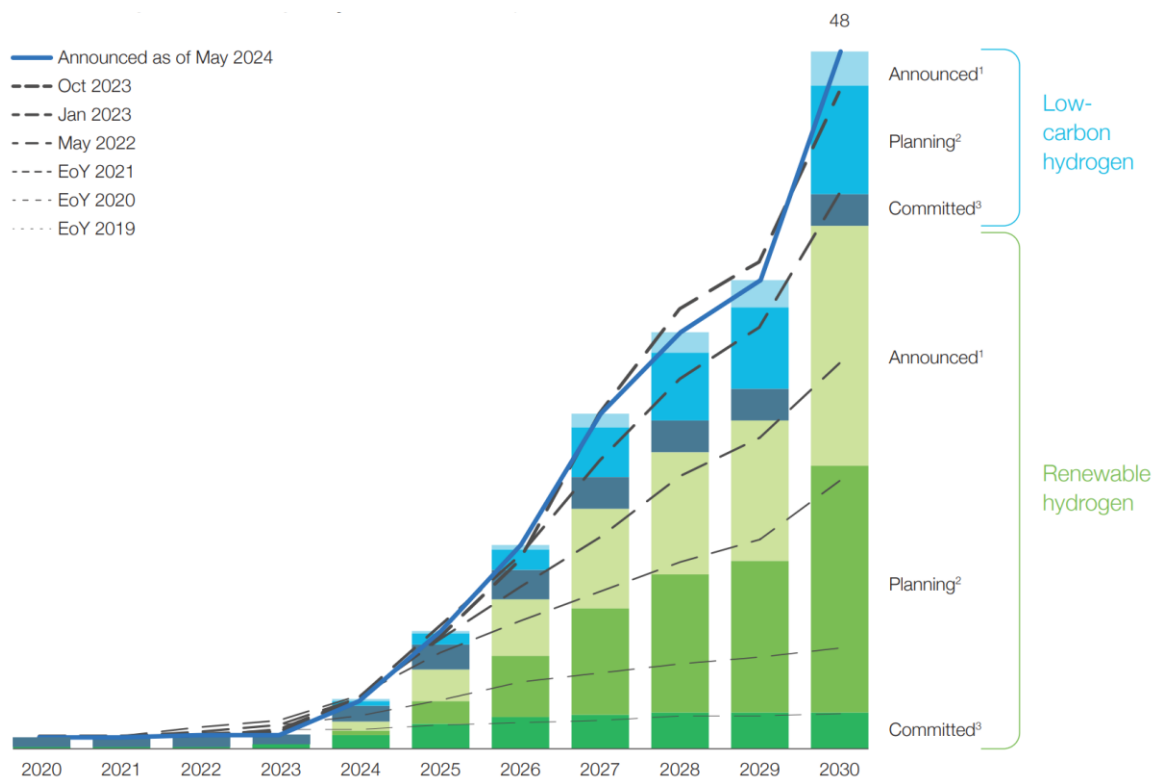


Figure 2. Cumulative production capacity [Mt p.a] for announced (1), planned (2) and committed (3) hydrogen projects (McKinsey & Company, 2024).

Companies have announced hydrogen projects for production of 48 Mt per annum for year 2030, where the development curve can be seen growing rapidly. 75% of announced projects are based on renewable energy source, which corresponds to 36 Mt annual production

capacity. 9% of announced projects have reached the final investment decision (FID) by end of 2024. Percentual part of the renewable hydrogen projects appears bigger already in 2025 based on Figure 2. Because the hydrogen production can be assessed as an energy intensive production, it's also interesting to review the announced projects with power units. Figure 3 is presenting announced cumulative water electrolysis capacity in GW unit from year 2020 to 2030. (McKinsey & Company. 2024)

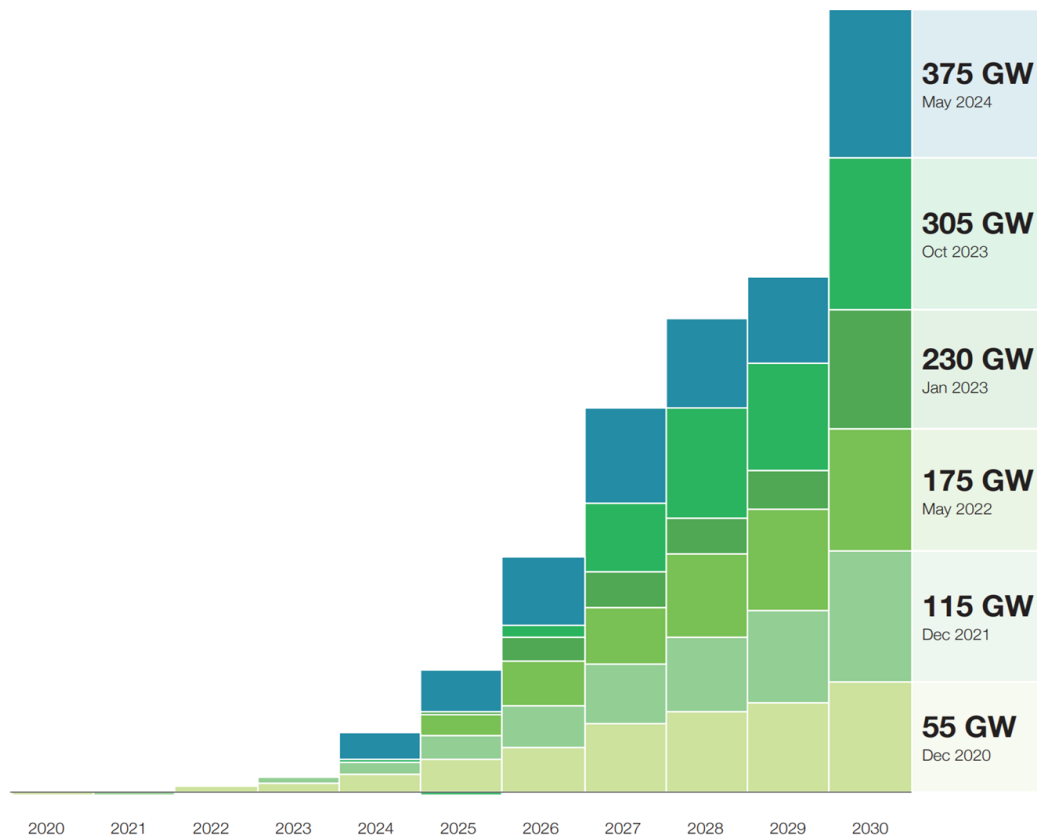


Figure 3. Announced cumulative electrolysis capacity [GW] from 2020 to 2030 (McKinsey & Company, 2024).

Total 375 GW electrolysis capacity has been announced where 160 GW is already under feasibility study or at front-end engineering design (FEED) phase. 26 GW of the electrolysis capacity has reached the FID. 105 GW of the total announced capacity is located in Europe, where 45 GW has reached at least a feasibility study phase. 30 GW of announced capacity is in North America and Latin America at 70 GW. Rest of the announced capacities are

located in Oceania at 50 GW, Middle East at 40 GW, India at 40 GW and rest of the world at 40 GW. (McKinsey & Company. 2024)

1.2 Green hydrogen at Helen Ltd

Helen is aiming to achieve 100% carbon neutrality in energy production. Helen's primary businesses are already district heating and cooling, electricity production, energy distribution and sales. (Helen, 2025a) Green hydrogen can help the energy transition where fossil fuel-based systems cannot be directly electrified, or energy storage is required on a large scale (Helen, 2025b). Green hydrogen production brings opportunities in addition to the current production solutions, where fluctuating electricity market prices can be exploited. Hydrogen projects are based on flexibility and energy efficiency, where in addition to the electricity market, the district heating market can be utilized, where the excess heat generated in electrolyzers can be utilized in the production of district heating. (Orkola et al. 2024) Hydrogen production can serve the transport sector as well as industrial customers, where Helen wants to be among the first for bringing the green hydrogen-based solutions available (Helen, 2025b).

1.3 Role of power distribution in the production of hydrogen in water electrolysis

Electrical energy is required 4 – 7.3 kWh for each produced hydrogen Nm^3 in water electrolysis depending on a type and manufacturer of the electrolyser (Guo et al. 2023). Electrolysers require DC power supply, so the rectifying equipment and power distribution plays a big role for the technology, where investment and plant operation periods are considered. The rectifier equipment are manufactured by using power electronic components, which can be seen as nonlinear load resulting harmonic distortion and possible reactive power. The nonlinear load produces harmonic currents, which are not only loading the power network but also flows to the network operator's grid causing voltage distortion and affects the other consumers as well. (IEEE 519-2022, 9) Grid code and standards give rules for power quality and engineering the plant distribution network, where selection of rectifier technology is a significant driver for the design. Limitation of harmonic distortion controls the selection of rectifier technology and possible filtering needs in the plant distribution network. Power grid

operators also have separated payments for reactive power which can be notable OPEX cost for the hydrogen production plant (Helen Sähköverkko, 2021).

Connection to the power grid should be investigated in early phase when preparing the water electrolysis project, not only for the total electrical power, but also the power quality should be considered. Too late findings for the poor electricity quality may cause delay for the project schedule due the equipment delivery times and also unexpected CAPEX and OPEX costs.

1.4 Previous studies

Differences between rectifier technologies has already been investigated in various studies. Previous studies have been investigating technologies for rectification and effects for the network as well as ripple in DC side. Studies gives theoretical applicability for understand the differences between the technologies and selecting rectifier units for the electrolyser systems.

(Keddar et al. 2022) is proposing 3-phase interleaved buck converter instead of thyristor-based converter for control 20 MW PEM electrolysis system. Improvement for power factor and THD is recognized especially in partial loads. The work is considering also ripple for DC power.

(Koponen et al. 2021) is comparing four different rectifier technologies including costs, where IGBT converter is suggested to improve the power quality for electricity network. Investment costs are higher compared to other technologies but annual costs of reactive power leads to saving by using the IGBT technology.

(Jakobsen et al. 2022) is proposing voltage source IGBT rectifier. IGBT technology eliminates the need of reactive power compensation but also the current is limited compared to the thyristor-based technologies. The converter with reactive power support can deliver reactive power to the grid, but with increased current where a current limiter is modelled.

(Zhao et al. 2023) has made simulation for 500 kW alkaline electrolyser system to analyse harmonics. Phase-shifted full bridge with active front end converter and passive filtering unit is selected for the simulation to supply the electrolyser. Simulation results indicate how short

circuit ratio affects the THD and how harmonics sidebands are affected by switching frequency and controller bandwidth.

1.5 Objectives, limitations and research questions

Large-scale electrolyser plants consist of multiple electrolyser units, where also multiple rectifying units are needed and power distribution appears complex. This master's thesis is examining, how the selection of rectifiers affects the power grid and how the hydrogen plant project should be managed to have a good technical solution, with considering power quality, reactive power and cost efficiency. Different load scenarios are selected to investigate the effects of a large-scale plant operating on power quality and reactive power. Hydrogen plant under the investigation should be connected to Helen Sähköverkko Oy's 110 kV power grid what gives requirements for the power quality and pricing for reactive power. Limit values from suitable standards are considered when reviewing compliance of the rectifier types and realistic power grid parameters are used in the simulations. OPEX costs are to be minimized, what gives requirements for the reactive power level defined by power grid operator. DC power quality of the rectifying units has not been investigated in the research. This thesis is limited to research only reactive power and harmonic distortion, and when referring to power quality, the meaning is in harmonic distortion. Research is considering only technologies what are already available in the market and request for quotation is assigned for power electronics suppliers. There are multiple other power consumers in the hydrogen plant which affects the power quality and reactive power in the distribution grid as well, which are not considered in this research.

Research questions for the thesis are: "What are the technical differences between rectifying technologies and how it affects genesis of the harmonic distortion and reactive power?" "How is the load and different load scenarios affecting the power quality and reactive power in a large-scale setup?" "What requirements are imposed on the transformer selection as a result of the rectifier selection?" "How are project CAPEX costs divided between different rectifier technologies in the project?"

1.6 Methods and structure

Both qualitative and quantitative research methods are utilized in this research. Budgetary quotation is requested for solve the suitable commercial converter solutions and to solve price division between the technologies. Also, theory section is processing the qualitative research questions and modelling of rectifier operation in large scale setup is processing the quantitative research questions. Standards and the grid code discussed gives limits for power quality in the modelling and power grid operator gives requirements for pricing the reactive power. ChatGPT by OpenAI is used for ensuring linguistic accuracy during the work.

Chapter 2 is presenting standards and power grid operator requirements utilized in this thesis. Chapter 3 is defining basis of electrolyser parameters and selection of rectifier technologies and topologies utilized. Theory part is explained in chapter 4 and simulations with simulation results are presented in chapter 5. Chapters 6 and 7 are presenting division for CAPEX costs between the technologies and proposed instructions for the project implementation. Conclusions are discussed in chapter 8.

2 Grid code and standards

Grid code and standards give requirements and recommendations for power quality in electricity networks. The grid code can vary from standards and it shall be taken into account when connecting loads to the public networks. The grid company also charges a fee for consumed or produced reactive power in 110 kV network (Helen Sähköverkko 2021).

2.1 Standards

Standard SFS-EN 50160:2022 gives recommendations for voltage characteristics in public electricity networks at the point of users supply terminals. The standard doesn't consider industrial networks but can be applied at the point of common coupling (PCC), which divides the network operator and electricity user at a certain voltage level. IEEE 519-2022 gives guidance for harmonic control in electric power system networks, which is especially intended for applications for unilinear load caused by power electronics. IEC 61000 standard series define widely electromagnetic compatibility in different environments. Standard SFS-EN 50160:2022 and IEEE 519-2022 are utilized in this research.

2.1.1 SFS-EN 50160:2022 Voltage characteristics of electricity supplied by public electricity networks

The standard SFS-EN 50160:2022 gives separate conditions for different voltage levels. For low voltage (LV) < 1 kV and for medium voltage (MV) level 1–36 kV conditions are the same and the conditions includes total harmonic distortion (THD) up to order 40 and individual limits for each harmonic voltages up to harmonic order 25. The SFS-EN 50160:2022 standard is not applied in this thesis at medium voltage side, because the MV network is defined as an industrial network and the actual PCC is at high voltage (HV) level.

According to the standard SFS-EN 50160:2022, voltage harmonic levels for high voltage 36–150 kV shall be selected lower compared to the medium voltage harmonic levels, what the network operator will eventually define. The allowed HV-value is indicated as difference

of MV-value and D , where the quantify D should be agreed between high voltage operator and the connected network user. The standard states:

“Under normal operating conditions, during each period of one week, 95% of min rms-values of each individual harmonic voltage should be less than the HV-value” (SFS-EN 50160:2022, 79)

The standard gives only indicative values for harmonic voltages at HV supply terminals and the values are presented in Table 1. (SFS-EN 50160:2022)

Table 1. Indicative values of individual harmonic voltages for HV voltage (SFS-EN 50160:2022)

Odd Harmonics				Even harmonics	
Not multiplies of 3		Multiplies of 3			
Order	Relative amplitude [%]	Order	Relative amplitude [%]	Order	Relative amplitude [%]
5	5.0	3	3.0	2	1.9
7	4.0	9	1.3	4	1.0
11	3.0	15	0.5	6-24	0.5
13	3.0	21	0.5		
17	-				
19	-				
23	-				
25	-				

Values that do not multiply of 3 for 17-25th harmonic components are under consideration (SFS-EN 50160:2022).

2.1.2 IEEE 519-2022 Standard of harmonic control in electric power systems

Standard IEEE 519-2022 can be utilized as guidance for engineering power systems which include non-linear loads such as, for example, rectifiers. The standard defines recommendations at the PCC, for example HV side of the transformer. (IEEE 519-2022)

The standard IEEE 519-2022 gives limits for total voltage distortion at PCC according to Table 2, where different limits are presented for different voltage levels.

Table 2. Voltage distortion limits for different voltage levels (IEEE 519-2022)

Voltage at PCC [kV]	Individual harmonic $h < 50$ [%]	THD [%]
< 1.0	5.0	8.0
1 - 69	3.0	5.0
69 - 161	1.5	2.5

The standard IEEE 519-2022 gives also limits for harmonic currents which are divided according to the voltage level. The standard states:

“Daily 99th percentile maximum 3 second harmonic currents shall be less than 2 times the values given in Tables 3 and 4. Weekly 99th percentile maximum 10 minutes harmonic currents shall be less than 1.5 times the values given in Tables 3 and 4. Weekly 95th percentile maximum 10 minutes harmonic currents shall be less than values given in Tables 3 and 4.” (IEEE 519-2022, 18)

The standard gives the ratio of harmonic currents distortion as a total demand distortion (TDD) instead of THD. The TDD is considering harmonic content up to the 50th order where the maximum demand load current I_L is used as a point of reference, what is the average maximum current considering 12 months. Table 3 defines current distortion limits for systems rated 120V to 69 kV and Table 4 defines current distortion limits for systems rated 69 kV to 161 kV. (IEEE 519-2022)

Table 3. Current distortion limits for systems rated 120 V to 69 kV (IEEE 519-2022)

Maximum harmonic current distortion in percent of maximum demand load current						
Individual harmonic order						
I_{sc}/I_L	$2 \leq h < 11$ [%]	$11 \leq h < 17$ [%]	$17 \leq h < 23$ [%]	$23 \leq h < 35$ [%]	$35 \leq h < 50$ [%]	TDD
< 20	4.0	2.0	1.5	0.6	0.3	5.0
20 < 50	7.0	3.5	2.5	1.0	0.5	8.0
50 < 100	10.0	4.5	4.0	1.5	0.7	12.0
100 < 1000	12.0	5.5	5.0	2.0	1.0	15.0
> 1000	15.0	7.0	6.0	2.5	1.4	20.0

Table 4. Current distortion limits for systems rated 69 to 161 kV (IEEE 519-2022)

Maximum harmonic current distortion in percent of maximum demand load current						
Individual harmonic order						
I_{SC}/I_L	$2 \leq h < 11$ [%]	$11 \leq h < 17$ [%]	$17 \leq h < 23$ [%]	$23 \leq h < 35$ [%]	$35 \leq h < 50$ [%]	TDD
< 20	2.0	1.0	0.75	0.3	0.15	2.5
20 < 50	3.5	1.75	1.25	0.5	0.25	4.0
50 < 100	5.0	2.25	2.0	0.75	0.35	6.0
100 < 1000	6.0	2.75	2.5	1.0	0.5	7.5
> 1000	7.5	3.5	3.0	1.25	0.7	10.0

Where I_{SC} is maximum short-circuit current at PCC and I_L is the maximum demand load current at PCC under normal load operating conditions. Even harmonic currents for $h \leq 6$ are limited to 50% from the values mentioned in Tables 3 and 4. (IEEE 519-2022)

2.2 Power quality in Fingrid's 110 kV grid

Helen Sähköverkko Oy is referring the Power quality in Fingrid's 110 kV grid report as requirement for Helen Sähköverkko Oy's 110 kV power grid (Heikkinen, 2024). The report defines allowed voltage harmonics in 110 kV grid side what electricity users shall be aware of. The report also defines emission current limits for feeding of currents with higher frequency than the fundamental to the power grid. (Fingrid, 2015)

2.2.1 Harmonics in 110 kV power grid

The maximum values of harmonic voltages are evaluated as 10-minute averages during a one-week period, where 99 percent of values shall be below the values given in Table 5. The total voltage harmonic distortion shall be below 3% and values are compared to the nominal voltage. (Fingrid, 2015).

Table 5. Maximum levels of individual harmonic voltages in Fingrid's 110 kV network
(Fingrid, 2015)

Harmonics do not multiply of 3		Harmonics multiplies of 3		Even harmonics	
Harmonic number	[%]	Harmonic number	[%]	Harmonic number	[%]
5	3.0	3	3	2	1.0
7	2.5	9	1.3	4	0.7
11	1.7	15	0.5	6	0.5
13	1.7	21	0.5	> 6	0.3
17	1.5	> 21	0.3		
19	1.5				
23	0.8				
25	0.8				
> 25	0.5				

As shown in Table 5, the Fingrid's maximum levels of harmonic voltages are lower compared to the standard SFS-EN 50160:2022 indicative values.

Fingrid sets maximum emission current limits for connecting parties. The maximum value of total harmonic current distortion is 6% and maximum psophometric value of phase current is 5 A. The percentual value refers to the per cent of connecting party's reference current. The reference current is calculated according to average active power, nominal voltage and using power factor 1 at the connecting party's grid connection. Psophometric value of phase current (I_p) is calculated according to equation 1.

$$I_p = \frac{1}{1000} \sqrt{\sum_{h=1}^{h=N} (p_h I_h)^2} \quad (1)$$

where I_h is harmonic component of phase current, h is harmonic order, N is number of harmonics included in the calculation, where 100 is used, p_h is frequency weighting coefficient at harmonic h . Psophometric weighting factors are presented in Appendix 1. (Fingrid, 2015)

2.3 Implementation of standards

Different standards and Fingrid's report give different values for harmonic limits, which may cause confusions. Voltage harmonics at the PCC are caused by current harmonics supplied to the grid together with impedance in the grid, which makes the current harmonics as a root cause for harmonic distortion. Applicable standards can be followed to evaluate maximum levels of harmonics, but the power grid operators might have more strict requirements what needs to be primarily followed.

2.4 Reactive power payments

Helen Sähköverkko Oy is charging their customers a fee from both reactive power and reactive energy at 110 kV power grid connection. Invoicing of reactive electricity is not charged from the 50 highest peaks, what exceeds the specific monthly free limit. Intake and output of reactive energy are invoiced from exceeding the free lot and the intake of reactive power is charged from the highest hourly peak in a month, from where 16% of active power measured at the same hour is subtracted. Respectively, the output reactive power is charged from the highest hourly peak, but 4% of the active power part is subtracted. A customer-specific fixed minimum amount of free reactive electricity is contracted with customers. (Helen Sähköverkko, 2021)

3 Electrolyser parameters and selection of rectifier types

The most common industrial electrolyser types are Alkaline (AEL) and Proton Exchange Membrane (PEM) where the Alkaline is the most mature technology. Differences between the technologies are due to the structure and materials used in membrane, electrolyte and electrodes, which also affects other equipment required for the electrolysis system. (Guo et al. 2023) Electrolyser technology was selected for the thesis, where parameters are needed for suitable rectifier selection. Used parameters are based on a PEM electrolyser, where cell voltage as a function of current density is used to model a working setup with the certain cell amount and surface area. The number of series connected cells are affecting the required total voltage over the electrolyser stack. Flowing current through the electrolyser stack is dependent on the surface area of the stack. (Nafchi et al. 2019)

3.1 PEM water electrolysis

PEM technology allows higher current density and efficiency as well as higher purity of the hydrogen compared to AEL technology. PEM electrode is manufactured from precious metals, which increases costs of the electrolyser and stack lifetime is also shorter compared to the alkaline electrolyser. Process flow of PEM water electrolysis is presented in Figure 4. (Guo et al. 2023)

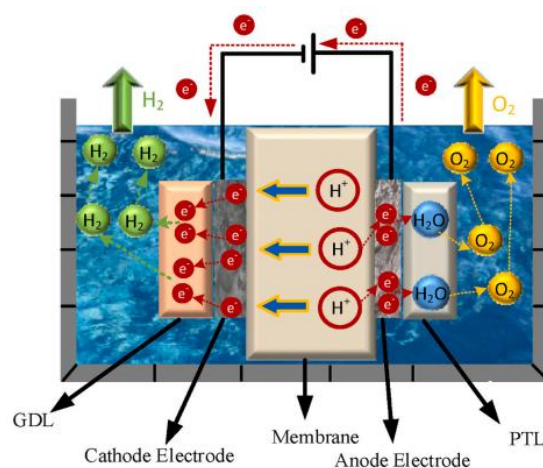


Figure 4. Process flow of PEM water electrolysis (Guo et al. 2023).

Structure of proton exchange membrane isolates the gases between the cathode and anode and conducts protons. The anode side breaks 1 mol of water into proton H^+ , electron e^- and 0.5 mol of oxygen. (Guo et al. 2023) Protons are transferred through the membrane to the cathode side where they unite for hydrogen and at the same time the electrons exit the electrolyser from electrical circuit, what provides the reaction. Porous transport layer (PTL) serves as an interface between the anode electrode and the water flow. Gas diffusion layer (GDL) focuses on release the hydrogen gas from the catalyst surface. (Nafchi et al. 2019)

3.2 Electrolyser parameters

Selected PEM electrolyser parameters are based on cell voltage as a function of current density according to Figure 5. The figure presents the values only for one cell what are later multiplied according to number of cells and surface area. (Nafchi et al. 2019)

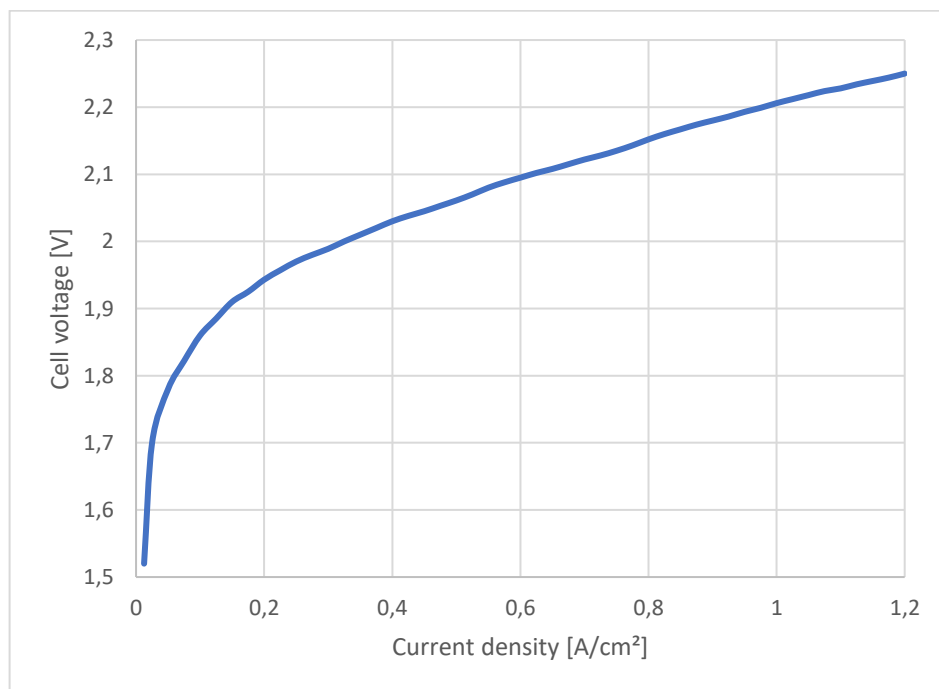


Figure 5. Cell voltage as a function of current density (Nafchi et al. 2019).

To get a simple even number for the stack power, the power for one stack was selected approximately to 1 MW, where the stack is selected to be built by 120 number of cells and

area of the stack is set to 3117.3 cm². Five stacks are connected in series to reach a 5 MW setup for the electrolyser and several 5 MW units are intended to connect to the grid to reach the desired total power of a water electrolysis plant. The cell voltage / current density curve with the presented selections and assumptions leads to the electrolyser parameters available in Table 6. Operational area of the electrolyser power is assumed to be approximately from 1 to 5 MW where the current density is between 0.275 and 1.2 A/cm² and cell voltage is between 1.989 and 2.258 V. Structure of the defined electrolyser is presented in Figure 6.

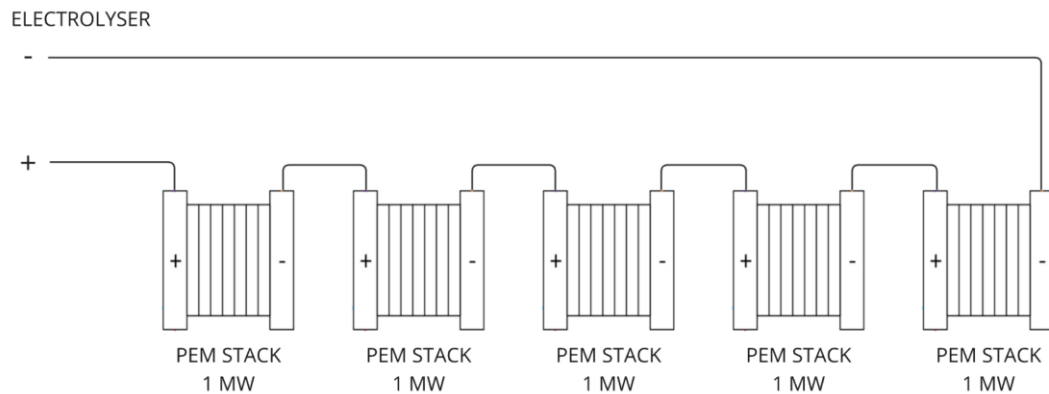


Figure 6. Structure of the defined electrolyser with five series connected PEM stacks.

Table 6. Electrolyser and grid parameters

Quantity	Value
DC Voltage min	1193 V
DC Voltage nominal	1355 V
DC Current min	857 A
DC Current nominal	3741 A
DC power min	1.02 MW
DC power nominal	5.07 MW
DC Voltage ripple max	3%
Medium voltage level	20 kV

The electrolyser parameters were used to investigate suitable rectification equipment from commercial power converter suppliers. Electrolyser manufacturers set the maximum DC voltage ripple level to have better efficiency and limit the degradation of the electrolyser

stacks, which is assumed to be 3% in this application (Keddar et al. 2022). The medium voltage level is needed for power converter suppliers to define a sufficient transformer for the application and suppliers were responsible for defining the secondary voltage of the transformer.

3.3 Selection of rectifier types

Rectifier types for further investigation were selected according to the budgetary quotations received from power electronics suppliers, where the electrolyser parameters from chapter 3.2 were utilized as initial data. Maximum value of harmonic distortion current THDi 5% was also set as initial data in the request of quotation. Power electronics suppliers proposed two individual rectifier technologies for the defined application, which were also selected for the further investigation of this research. The first converter proposed is based on a thyristor technology, where the topology is presented in Figure 7.

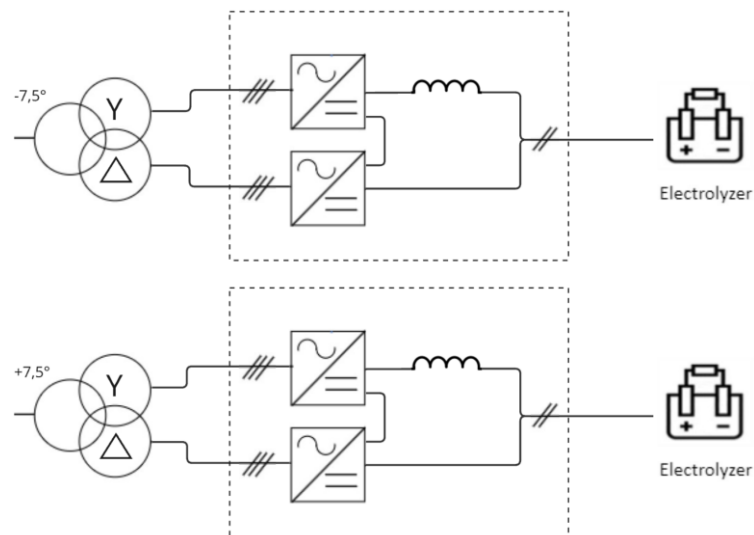


Figure 7. Proposed 24-pulse thyristor rectifier topology with DC reactors.

The proposed thyristor rectifier topology includes two sets of 12-pulse thyristor bridge converters, where the supply transformers have 15 degrees phase shift between the primaries. Each of the 12-pulse rectifiers includes series connected pair of 6-pulse thyristor bridges. The proposed transformers are 20/0.568/0.568 kV three winding transformers, where also

30 degrees phase shift between the secondary and tertiary windings is used. Secondary and tertiary windings have also delta-wye connection differences. The topology appears to be a 24-pulse thyristor rectifier to the power grid because of connection and phase shifts mentioned, but also the identical load is required for both units. Reactors are utilized at DC side of the converters to reduce harmonic currents at AC side.

The second technology proposed is insulated-gate bipolar transistor (IGBT) based active front end converter, where two converters are parallel connected. The proposed IGBT rectification topology is presented in Figure 8.

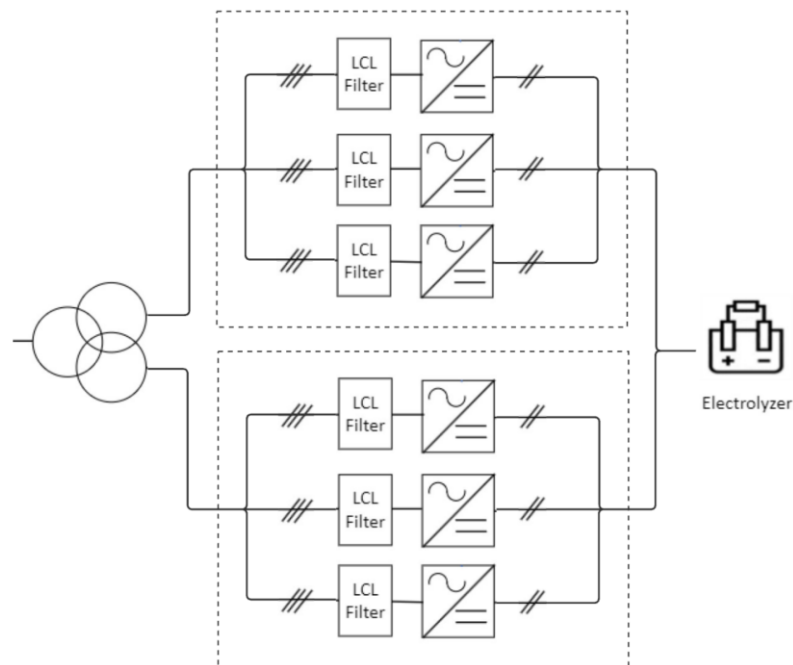


Figure 8. Proposed IGBT rectifier topology with LCL filters.

Both converters include three parallel sets of IGBT bridges with LCL filters. Parallel bridges and converters are required due to the limitations of the current withstanding of power electronics. Transformers proposed are 20/0.69/0.69 kV three winding transformers and no special vector group or phase shifting is required.

4 Rectifier technologies

Rectifier types for the research were selected according to budgetary quotations received from power electronics suppliers based on the defined electrolyser parameters. This chapter describes technologies, principles for control and genesis of harmonics and reactive power. Only three phase rectifiers are investigated, hence the thesis considers only MW power class equipment.

4.1 Thyristor bridge rectifiers

Thyristor based rectifiers are suitable for high power applications, but pure thyristor-based applications are comparatively inefficient with the harmonic distortion and power factor (Koponen et al. 2021). Harmonic distortion can be improved by utilizing multi-pulse bridges (ABB, 2017).

4.1.1 Thyristor bridge rectifier topologies

6-pulse thyristor rectifier is a topology, where six gate-controlled thyristors are connected as a bridge. There are no special vector group requirements for transformers when utilizing the 6-pulse topology. (Koponen et al. 2021) The 6-pulse topology is presented in Figure 9.

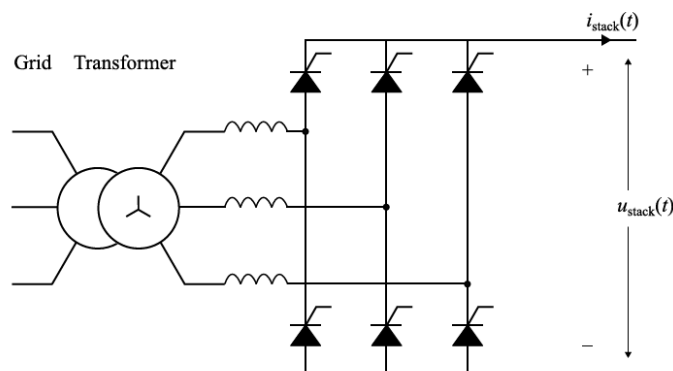


Figure 9. 6-pulse thyristor rectifier topology (Koponen et al. 2021).

Better characteristics for harmonic distortion can be achieved by parallel or series connected thyristor bridges. The structure is more complex and there is also a need for multiple windings for the grid transformer depending on the number of bridges connected. Three winding transformers are used for 12-pulse bridge thyristor rectifiers, where secondary coil is delta-connected and tertiary coil is wye-connected. The transformer generates 30 degrees phase shift between the two bridges. (Koponen et al. 2021) The 12-pulse topology is presented in Figure 10.

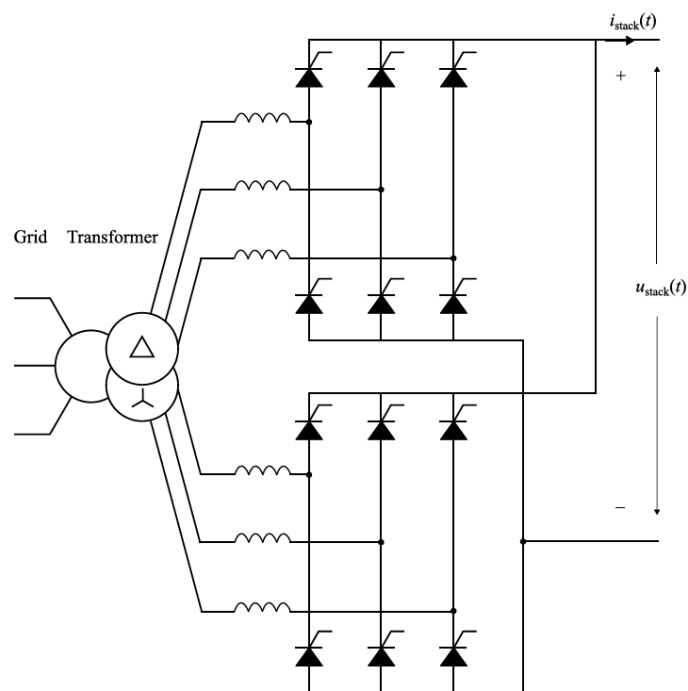


Figure 10. Parallel connected 12-pulse thyristor rectifier topology (Koponen et al. 2021).

4.1.2 Control and characteristics of 6-pulse thyristor bridge rectifier

The output power can be controlled by a thyristor bridge converter. Thyristor-based equipment are line-commutated rectifiers where thyristor states are switched ON and OFF only once per sine wave cycle. Adjusting firing delay angle α sets timing for thyristor control to manipulate the grid sine wave and limit power from DC side. The firing delay angle α is measured from the phase voltages crossing point, which can be seen from Figure 11. The

thyristor bridge works as a diode bridge with $\alpha = 0^\circ$ firing angle control. Increasing the firing angle the output power is decreased until the firing angle is 90° . (Mohan et al. 2003)

Neglecting inductances and assuming DC current to be constant, the ideal 6-pulse bridge thyristor rectifiers average DC voltage can be calculated according to equation 2 and dependence of the firing delay angle α is noticeable.

$$V_D = \frac{3\sqrt{2}}{\pi} V_{LL} \cos \alpha \quad (2)$$

where V_{LL} is RMS value of line-to-line AC voltage. (Mohan et al. 2003) The average power of the ideal six pulse thyristor bridge can be calculated according to equation 3.

$$P = V_D I_D = 1,35 V_{LL} I_D \cos \alpha \quad (3)$$

where I_D is DC current. Input phase currents for the ideal rectifier have rectangular shapes and amplitude as I_D . The firing delay angle causes a phase shift for input current and has effect for power factor for AC side of the thyristor bridge converter. Power factor (PF) for the ideal 6-pulse rectifier can be calculated according to equation 4 and dependence of the firing delay angle α can be observed. (Mohan et al. 2003)

$$PF = \frac{3}{\pi} \cos \alpha \quad (4)$$

The phase shift for ideal 6-pulse rectifier can be seen from Figure 11, where the phase current i_a is lagging voltage V_a by angle Φ_1 because of the firing delay angle α . (Mohan et al. 2003)

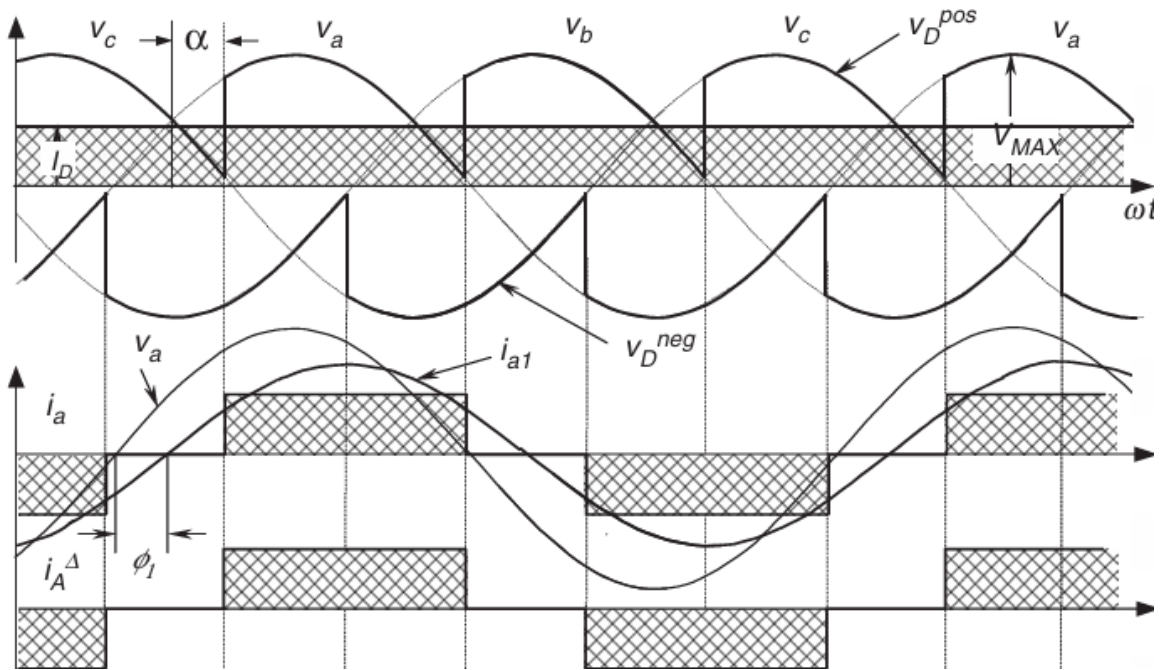


Figure 11. Phase current i_a lagging the voltage V_a by angle Φ_1 because of the firing delay angle α (Rashid, 2011).

As shown in Figure 11, the current at A-phase starts conducting after the firing delay angle ends and affects the reactive power by phase shift angle Φ_1 . Status in Figure 11 is assumed to have such a large inductance in the DC loop that the DC current I_D is constant.

Due to converter characteristics the input AC current is not fully sinusoidal and will have harmonic content according to Fourier series presented in equation 5.

$$i_A = \frac{2\sqrt{3}}{\pi} I_D (\sin \omega t + \frac{1}{5} \sin 5\omega t + \frac{1}{7} \sin 7\omega t + \frac{1}{11} \sin 11\omega t + \dots) \quad (5)$$

where ωt is angular frequency at a moment of time. Only non-triplen odd harmonics exist with the presence of harmonic order $6n \pm 1$. (Mohammed et al. 2019) The RMS value for rectifier fundamental phase current can be expressed according to equation 6.

$$I_1 = \frac{\sqrt{6}}{\pi} I_D \quad (6)$$

The RMS value of each harmonic current can be calculated according to equation 7.

$$I_n = \frac{I_1}{n} \quad (7)$$

where n is non-triplen harmonic number $6n \pm 1$ and where n is (1,2...). Non-sinusoidal AC currents have also negative effects for converter power factor. Increased distortion in current also increases the value of I_a^{rms} which affects the PF according to equation 8.

$$PF = \frac{I_{a1}^{\text{rms}}}{I_a^{\text{rms}}} \cos \alpha \quad (8)$$

where I_a^{rms} is the RMS value the phase current i_a and I_{a1}^{rms} is the RMS value of fundamental component of the phase current i_a . (Rashid, 2011)

When using a transformer where either of the windings is delta connected, positive $6n + 1$ and negative $6n - 1$ sequence order harmonic current angles rotate and results Fourier series for transformers primary side phase current according to equation 9 (Rashid, 2011).

$$i_A = \frac{2\sqrt{3}}{\pi} I_D (\sin \omega t - \frac{1}{5} \sin 5\omega t - \frac{1}{7} \sin 7\omega t + \frac{1}{11} \sin 11\omega t + \dots) \quad (9)$$

AC side inductance L_s is present with practical rectifiers, where inductance of transformers plays a big role. The presence of the inductance L_s causes an overlap angle μ where two thyristors are conducted at the same time and causes two phases shorted together via inductance L_s in each commutation cycle. The overlap angle μ is dependent on phase-to-phase voltage and inductance L_s in the AC grid. DC current with considering the overlap angle μ can be calculated according to equation 10. (Rashid, 2011)

$$I_D = \frac{V_{LL}}{\sqrt{2}\omega L_s} [\cos \alpha - \cos(\alpha - \mu)] \quad (10)$$

The commutation overlap angle μ causes drop of DC voltage which reduces the average DC voltage and can be calculated according to equation 11. (Rashid, 2011)

$$V_D = \frac{3\sqrt{2}}{\pi} V_{LL} \cos \alpha - \frac{3\omega L_s}{\pi} I_D \quad (11)$$

Effects of the overlap angle μ for the voltages and currents are presented in Figure 12.

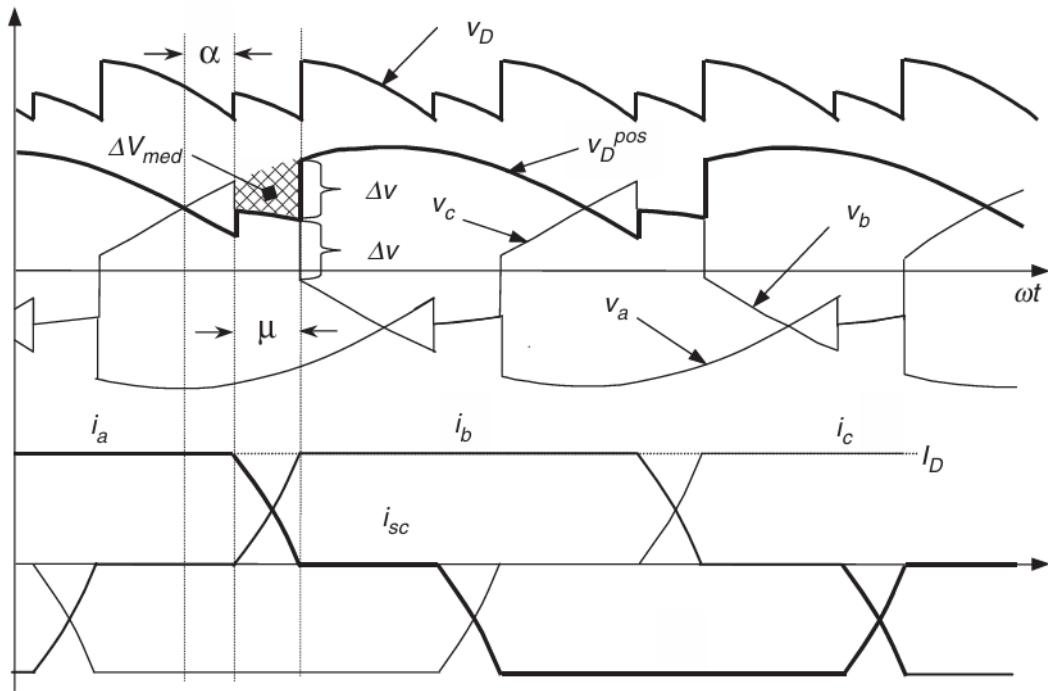


Figure 12. Overlap angle μ and effect for the voltages and currents (Rashid 2011).

As shown in Figure 12, the phase currents are not anymore rectangular because of the overlap angle and two of phase currents are conducting at the same time during the overlap angle. Effects of the overlap angle are also visible at the DC voltage U_D as well as phase voltages. The overlap angle μ reduces also converter power factor by increasing the displacement power factor (DPF) according to equation 12 where the waveform for current i_a is approximated to be trapezoidal. Although the overlap angle is causing instability for the operation, the presence of inductance L_s has reducing impact on harmonic current magnitudes. (Mohan et al. 2003)

$$DPF \cong \cos\left(\alpha + \frac{1}{2}\mu\right) \quad (12)$$

4.1.3 Benefits of multi-pulse thyristor bridge configurations

With 12-pulse topology, the input current forms the sum of star and delta connection transformers in a Fourier series. With the 12-pulse configuration, the harmonic currents of order $6n \pm 1$ circulates only between the transformer secondary and tertiary coils, but these harmonics can't access the MV network side of the transformer. Only harmonic currents of

order $12n \pm 1$ can penetrate the transformer and thus improve the power quality. The Fourier series for the primary side of the transformer in 12-pulse operation can be expressed as presented in equation 13, which is the sum of star connection Fourier series and delta connection Fourier series. (Rashid, 2011)

$$i_A = 2\left(\frac{2\sqrt{3}}{\pi}\right)I_D(\sin \omega t + \frac{1}{11}\sin 11\omega t + \frac{1}{13}\sin 13\omega t + \frac{1}{23}\sin 23\omega t + \dots) \quad (13)$$

The topology is not limited to 12-pulses, but also higher pulse configurations can be used. Even better characteristics for harmonic distortion are achieved for example with 18- or 24-pulse rectifiers, where the topology is more complex and requires more secondary windings from the grid transformers (Rashid, 2011). The 24-pulse topology can be also constructed by utilizing two parallel 12-pulse converters supplied by transformers, where the primary windings are phase shifted 15 degrees relative to each other. The load for both 12-pulse units shall be identical to appear the 24-pulse operation towards the power grid. (ABB, 2017) The Fourier series for 24-pulse operation can be expressed as a sum of two 12-pulse rectifiers, where the other is following equation 13 and other is following equation 14 because of the phase shift between the transformer primaries.

$$i_A = 2\left(\frac{2\sqrt{3}}{\pi}\right)I_D(\sin \omega t - \frac{1}{11}\sin 11\omega t - \frac{1}{13}\sin 13\omega t + \frac{1}{23}\sin 23\omega t + \dots) \quad (14)$$

Fourier series for 24-pulse operation results according to equation 15.

$$i_A = 4\left(\frac{2\sqrt{3}}{\pi}\right)I_D(\sin \omega t + \frac{1}{23}\sin 23\omega t + \frac{1}{25}\sin 25\omega t + \frac{1}{47}\sin 47\omega t + \dots) \quad (15)$$

where opposite polarity per cycle has been cancelled out. (Mohammed et al. 2019)

Comparison for waveforms in 6-, 12- and 24-pulse operations is presented in Figure 13, where the currents are measured from primary side of the transformers.

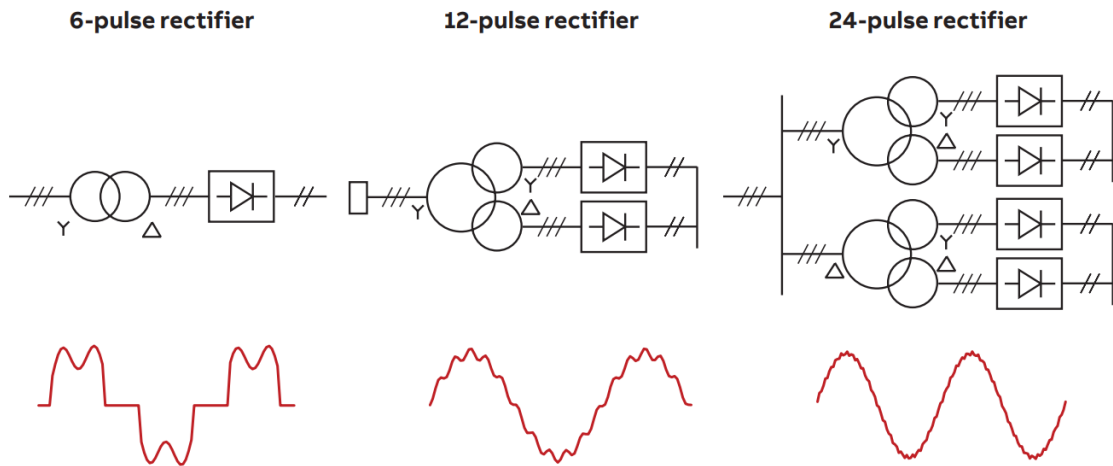


Figure 13. Input phase current waveforms for 6-pulse, 12-pulse and 24-pulse thyristor/diode bridge rectifiers (ABB, 2017).

The input phase currents in multi-pulse converter operation will have waveforms which are closer to sinusoidal shape when comparing to 6-pulse configuration (Rashid, 2011). The PF of the multi-pulse configuration is slightly improved compared to the 6-pulse converter due to the lower harmonic currents (Koponen et al. 2021). Relation to power factor of harmonic currents is presented in equation 8. DC-voltage level for the series connected 12-pulse rectifier is doubled from the 6-pulse converter, which needs to be considered in rectifier transformers transforming ratio.

4.2 IGBT rectifiers

Insulated-gate bipolar transistor (IGBT) rectifiers are active force-commutated converters, where the transistor ON and OFF states can be controlled by pulse-width modulation (PWM) and achieve improved characteristics of harmonic distortion and power factor. Due to the control method, the power factor can be controlled, or reactive power can be even produced towards the power grid. Performance limitations in the IGBT power converters are based on the maximum allowed current for the IGBT bridge modules, what leads the need to connect several converters in parallel in high power applications. Controlling the IGBT converter requires sensors for both AC and DC sides and the control philosophy is more complex

compared to the thyristor converters (Rashid, 2011). The structure of a voltage source IGBT rectifier with LCL filter is presented in Figure 14.

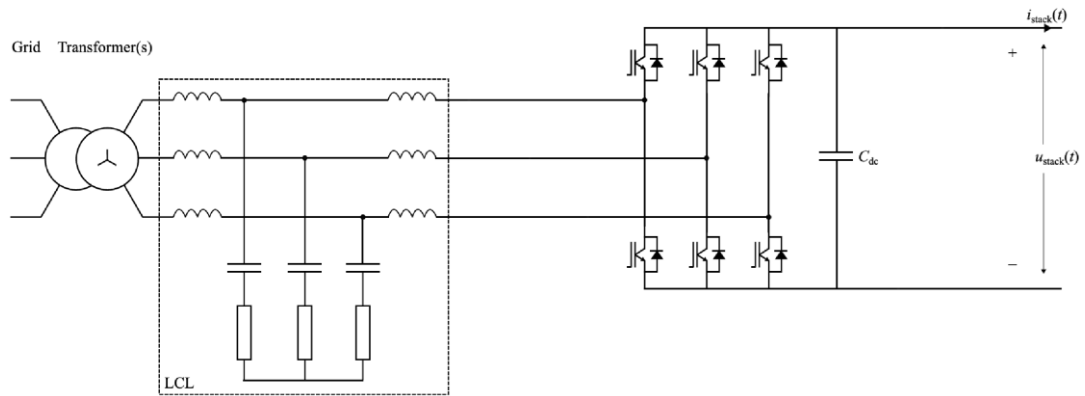


Figure 14. IGBT rectifier with LCL filter (Koponen et al. 2021).

As shown in Figure 14, a passive filter is used on the AC side of converter. Typical active PWM rectifiers operates switching frequencies between 2 to 15 kHz, which can cause high-order harmonics to the power grid. These harmonics typically occur around the switching frequency and can be reduced by adding a high inductance value at input of the rectifier. However, this can lead to poor dynamic response and may not be a financially efficient solution. Harmonic reduction can be achieved with a lower inductance value by utilizing an LCL filter. (Liserre et al. 2005) Dimensioning of the LCL filter is discussed in chapter 5.6.1.

4.2.1 PWM modulation

Different methods are available for producing the PWM pattern for IGBT transistors. This thesis is presenting the sinusoidal pulse width modulation (SPWM) method, where the PWM pattern is based on voltage reference V_{MOD} , which follows the grid frequency. The reference waveform V_{MOD} together with the symmetrical triangular carrier wave V_{TRIANG} defines the switching points for each transistor. With this method, the PWM pattern follows the amplitude and phase of V_{MOD} as presented in Figure 15, where the operation of one phase-leg is presented. (Rashid, 2011)

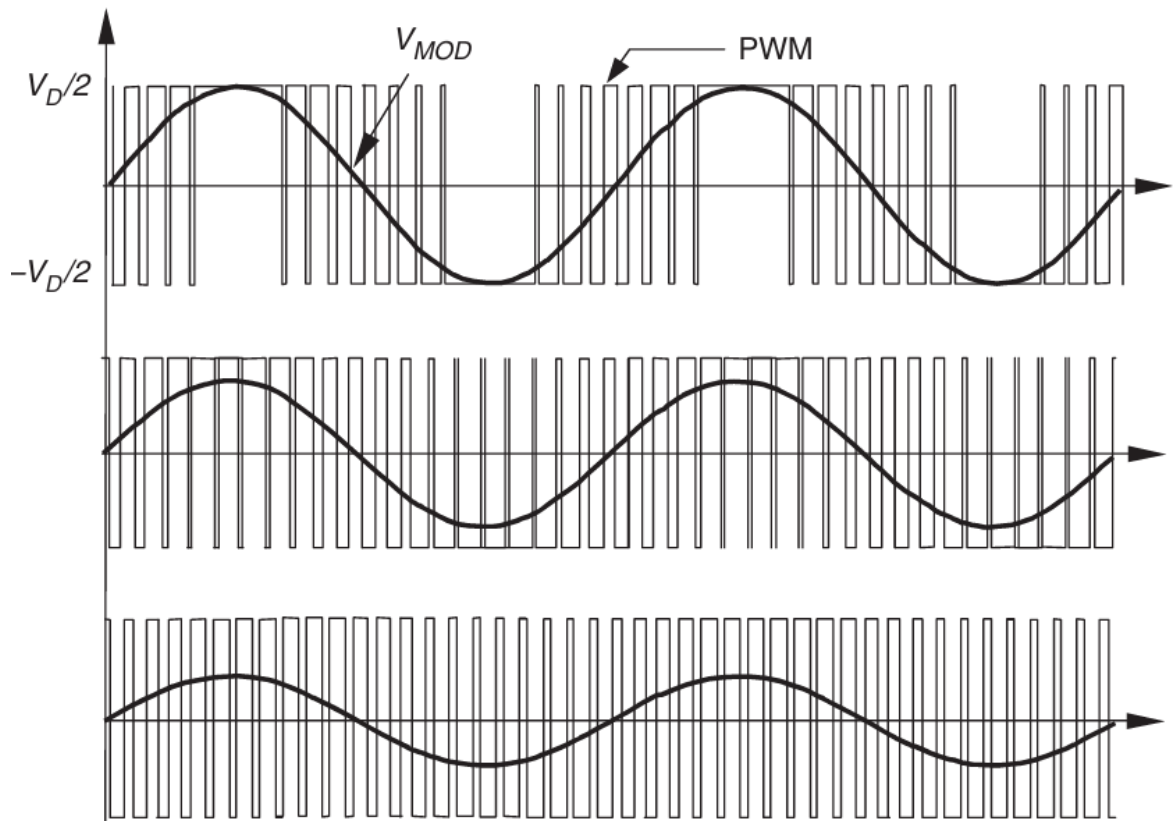


Figure 15. PWM pattern follows the reference V_{MOD} amplitude, phase and frequency (Rashid, 2011).

As shown in the Figure 15, the PWM pattern follows the reference signal and therefore controls the converter DC voltage. In other words, the reference signal amplitude shall be controlled to adjust the rectifier DC power. The active bridge converter can also control the reactive power by shifting the V_{MOD} reference signal phase compared to the mains phase, which also displaces the PWM signal. Equation 16 can be utilized to define the reference V_{MOD} as a function of time with unity power factor operation $\cos\phi = 1$.

$$v_{MOD}(t) = (V\sqrt{2} - RI_{max} - L_s \frac{dI_{max}}{dt})\sin(\omega t) - \omega L_s I_{max} \cos(\omega t) \quad (16)$$

where V is source voltage, I_{max} is input current amplitude for the converter, R is resistance in AC grid side and L_s is inductance in AC side. The in-phase term $\sin(\omega t)$ and the in-quadrature term $\cos(\omega t)$ together allows adjusting the reference amplitude and phase to achieve the unity power factor operation. (Rashid 2011)

The carrier wave V_{TRIANG} defines the actual switching points of the transistors, so the switching frequency is defined by frequency of the carrier. Figure 16 presents the PWM pattern for one phase-leg compared to the reference V_{MOD} and carrier V_{TRIANG} waveforms, as well as phase A to neutral PWM voltage measurement. (Rashid, 2011)

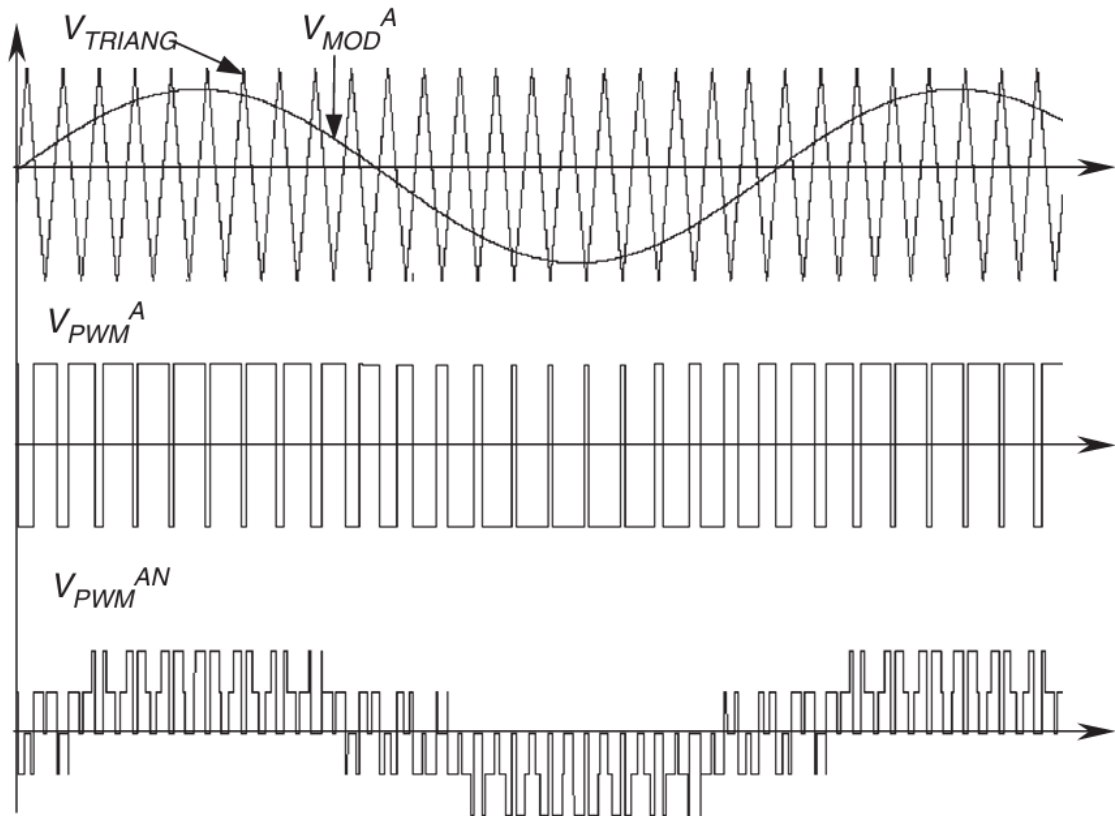


Figure 16. PWM pattern compared to the reference V_{MOD} and carrier V_{TRIANG} waveforms and phase A to neutral PWM voltage measurement (Rashid, 2011).

Upper transistor of the phase-leg is controlled ON when the reference signal is higher than the carrier and at the same time the lower transistor is respectively controlled OFF. All three phase legs use the same carrier wave, but the reference waveforms are separated for each phase due to the three-phase system, which defines suitable switching points for all phases.

Modulation index m is defined as the ratio of maximum values of V_{MOD} and V_{TRIANG} . When the $m > 1$, overmodulation happens, which means that the reference voltage amplitude is not increased anymore linearly, and harmonic content is increased. Frequency modulation ratio

p is defined as the ratio of carrier frequency and mains frequency. It is recommended to keep the frequency modulation ratio as an integer to avoid subharmonics. Also, it is recommended to keep the frequency modulation ratio as an odd number to avoid even harmonics. To keep the PWM modulation identical for all three phases, the frequency modulation ratio should be multiple of 3. Because the p is defined as the ratio of carrier frequency and mains frequency, increasing the value of p will increase also the switching frequency and harmonic content of the input current is decreased. (Rashid, 2011)

Harmonic content can be decreased more by connecting several IGBT bridges in parallel or series, which is commonly utilized in high power applications. Modulating carriers for each bridge can be phase-shifted to cancel harmonics from the total setup. Shifting angle δ_T of the carriers depends on the number of converters used in the setup according to equation 17.

$$\delta_T = \frac{2\pi}{n} \quad (17)$$

where n is the number of converters connected. (Rashid, 2011)

5 Modelling of rectifier operation

The rectifier operation was simulated by using Matlab® and Simulink® software, where the Simscape™ library was utilized. Separated models were made for thyristor and IGBT transistor operations with identical DC load to compare the power quality between the technologies used. The DC load follows the PEM electrolyser current and voltage presented in chapter 3, and three load points were selected to demonstrate the dependence on power quality. Topologies for rectifiers follow the budgetary quotations received from power electronics supplier, which are requested according to defined electrolyser and power grid parameters. Parallel electrolyser/rectifier units are connected to the medium voltage grid to simulate a 50 MW electrolyser plant, which consists of 10 units of 5 MW power electrolyser/rectifier systems in the model. The models include DC loop, rectifiers, rectifier transformers, LCL filters for IGBT units, main transformers and the power grid. Transformer coils comprise resistance and inductance to the network and affect reactive power and harmonic distortion. The inductance is filtering harmonic distortion, but it's also consuming reactive power what should be noticed in electrical engineering. Transformers short circuit impedance parameters can also be used to limit the short circuit current at the secondary side. Switchgears, cables and busbars etc. are not considered in the model. Electrical parameters of the actual thyristors and IGBT transistors are based on Simulink block initial values and the power grid doesn't have any existing voltage distortion. Simulation models of rectifiers don't fully correspond to the commercial equipment because all parameters are not known from the power electronics and control methods.

5.1 DC load

The DC load is simulated by using a constant current source, where the current value is selected according to desired operation point and the DC voltage is controlled by rectifiers. The DC power is represented as the product of DC current and voltage.

5.2 Power grid parameters

The investigated electrolyser plant is planned to be connected to a 110 kV power grid, where realistic parameters of the 110 kV grid have been used in the Simulink model. In addition to the grid voltage, the short circuit power and the ratio of grid resistance to reactance are defined in the model. The short circuit power is based on equation 18.

$$I_k = \frac{1,1S_k}{\sqrt{3}U_{LL}} \quad (18)$$

where I_k is short circuit current, S_k is short circuit power, U_{LL} is phase to phase voltage and 1.1 is a factor based on maximum short circuit current calculation (ABB, 2000). The short circuit power at the power grid can be evaluated also as a stiffness of the network. When the power grid is stiff, the network can serve the required current and voltage easier without affecting interference. (McGraw, 2025)

5.3 Main transformer parameters

The transformer block in the Simulink model includes parameters for primary and secondary coil inductances and resistances as well as magnetizing inductance and resistance. Transformers nameplate values do not include directly the parameters mentioned, but most of the parameters can be approximated by utilizing the transformers nameplate values. The main transformer is transforming the 110 kV grid voltage to 20 kV medium voltage and the nameplate values are based on information received from a transformer manufacturer. Transformer nameplate values used in the approximation are presented in Table 7.

Table 7. Nameplate values for the main transformer

Quantity	Value
Nominal power S_n	110 MVA
Primary voltage U_1	118 kV
Secondary voltage U_2	21 kV
Load losses P_L	322 kW
No-load losses P_0	27 kW
Relative short circuit impedance U_k	16%
Vector group	YnD11

The transformers primary current I_1 is counted as the ratio of nominal power and primary voltage. Load losses refer to heat loss in the transformer windings caused by resistance. Short circuit resistance R_k can be calculated with known primary current and load losses according to equation 19. (Nerg, 2024)

$$R_k = \frac{P_L}{I_1^2} \quad (19)$$

The short circuit resistance is assumed to be split equally between the primary and secondary sides. However, the secondary side resistance R_2 is adjusted according to the transforming ratio by multiplying the resistance value by the square of the transforming ratio. The short circuit impedance must be calculated to define also the short circuit reactance. The short circuit impedance Z_k is calculated according to equation 20. (Nerg, 2024)

$$Z_k = U_k \frac{U_1^2}{S_n} \quad (20)$$

The short circuit reactance X_k is calculated by using Pythagoras according to equation 21. (Nerg, 2024)

$$X_k = \sqrt{Z_k^2 - R_k^2} \quad (21)$$

The reactance is fully inductive and is also assumed to be split equally between the primary and secondary sides. Similar way as the resistance, the secondary side reactance is reduced by multiplying the reactance value by the square of the transforming ratio. Inductance L_x of each winding is calculated according to equation 22 where the grid frequency 50 Hz is used, and reactance value X is used according to selected side of the transformer. (Nerg, 2024)

$$L_x = \frac{X_x}{2\pi f} \quad (22)$$

The no-load losses are caused by magnetization resistance R_m which can be calculated by utilizing equation 23. (Nerg, 2024)

$$R_m = \frac{U_1^2}{P_0} \quad (23)$$

Magnetization inductance L_m cannot be evaluated with the information available from transformers nameplate, but the inductance is assumed to be large (Nerg, 2024). Parameters used in the Simulink model for the main transformer are based on equations 19-23 and are presented in Table 8. -5% tapping is utilized in the transformer primary side for voltage control purposes, because other consumers are assumed to be connected also in the MV network, and the voltage level should be kept in 20 kV during the maximum load scenario.

Table 8. Parameters calculated for the main transformer according to the nameplate values

Quantity	Value
Primary resistance R_1	185.3 m Ω
Secondary resistance R_2	5.9 m Ω
Primary inductance L_1	32.2 mH
Secondary inductance L_2	2.0 mH
Magnetization resistance R_m	515.7 k Ω
Magnetization inductance L_m	200.0 H (estimated)

5.4 Parameters for rectifier transformers

Three-winding transformers are utilized in both Simulink models to supply low voltage power for the rectifiers. The three-winding transformers have tertiary winding in addition to the two-winding transformers and it shall be considered when estimating the parameters. Thyristor rectifier transformers nameplate values are presented in Table 9 and IGBT rectifier transformer values in Table 10.

Table 9. Nameplate values for the thyristor rectifier transformer

Quantity	Value
Nominal power S_n	6.01 MVA
Primary voltage U_1	20 kV
Secondary voltage U_2	0.568 kV
Load losses P_L	56 kW
No-load losses P_0	8 kW
Relative short circuit impedance U_k	8%
Vector group	$Y_n(+7.5)y0d1 + Y_n(-7.5)y0d1$

Table 10. Nameplate values for the IGBT rectifier transformer

Quantity	Value
Nominal power S_n	5.42 MVA
Primary voltage U_1	20 kV
Secondary voltage U_2	0.69 kV
Load losses P_L	51 kW
No-load losses P_0	7.6 kW
Relative short circuit impedance U_k	8%
Vector group	Y_{nd1d1}

In the transformers equivalent circuit, the secondary and tertiary windings of the three-winding transformer are connected in parallel. The parallel connections are taken into account for resistance and reactance calculations, after the short circuit resistance R_k and reactance X_k values are split equally for secondary side of the transformers. Additionally for the thyristor rectifier transformer, the secondary winding of the three-winding transformer is star-connected, while the tertiary winding is delta-connected. The resistance and reactance of the delta-connected winding are three times higher compared to the star-connected winding due to the connection difference. The IGBT transformer does not require different connections for the secondary side of the transformer and therefore the previous mentioned differences are not concerning the IGBT transformer. Parameters approximated for the thyristor rectifier transformers are presented in Table 11 and parameters approximated for the IGBT rectifier transformers are presented in Table 12. The parameters are based on equations 19-23.

Table 11. Parameters calculated for the thyristor rectifier transformer according to the nameplate values

Quantity	Value
Primary resistance R_1	310.08 m Ω
Secondary resistance R_2	0.33 m Ω
Tertiary resistance R_3	1.00 m Ω
Primary inductance L_1	8.42 mH
Secondary inductance L_2	9.04 μ H
Tertiary inductance L_3	27.10 μ H
Magnetization resistance R_m	50.00 k Ω
Magnetization inductance L_m	119.00 H (estimated)

Table 12. Parameters calculated for the IGBT rectifier transformer according to the nameplate values

Quantity	Value
Primary resistance R_1	347.22 m Ω
Secondary resistance R_2	0.83 m Ω
Tertiary resistance R_3	0.83 m Ω
Primary inductance L_1	9.33 mH
Secondary inductance L_2	22.20 μ H
Tertiary inductance L_3	22.20 μ H
Magnetization resistance R_m	52.63 k Ω
Magnetization inductance L_m	119.00 H (estimated)

5.5 Thyristor rectifier model

The thyristor rectifier design is based on similar 24-pulse topology as proposed in chapter 3.3. Topology without control signals for thyristor rectifying system is presented in Figure 17.

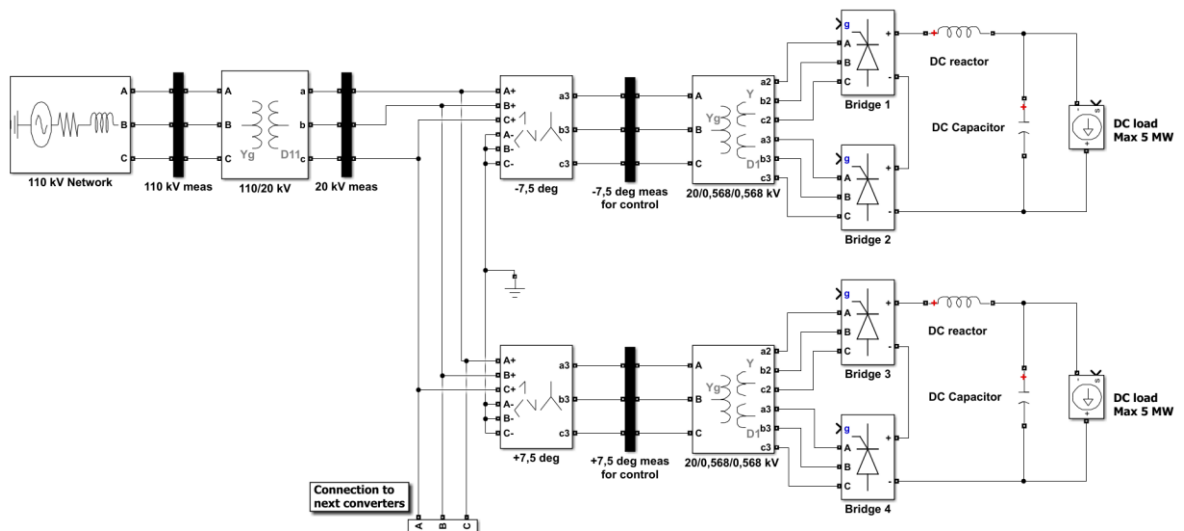


Figure 17. Topology of 24-pulse thyristor bridge rectifier and power network. The figure presents 10 MW DC load controlled by the thyristor converters.

The zigzag transformers at primary side of the three-winding transformers are used only for phase shifting purposes and resistances and inductances for coils are set to a minimum. Magnetization resistance and inductance are set very high to minimize the current is not consumed for magnetization in the zigzag transformer. Each series connected 12-pulse system serves a 5 MW DC load, where 20 mF DC capacitors are used to stabilize voltage ripple in the DC link. DC reactors 0.4 mH are used according to power electronics supplier's quotation which has a reducing effect on harmonic currents in the AC side. Measuring points are connected on each level of the circuit to have the information needed for control and measure also the performance of 24-pulse system. Five pieces of 24-pulse units are connected in parallel to the 20 kV medium voltage grid to have the simulation model of a 50 MW electrolyser plant. Maximum +8% tapping is utilized in rectifier transformers primary side for voltage control purposes to minimize the firing angle.

5.5.1 Control of thyristor bridge rectifier

Control philosophy of the 12-pulse converter is presented in Figure 18.

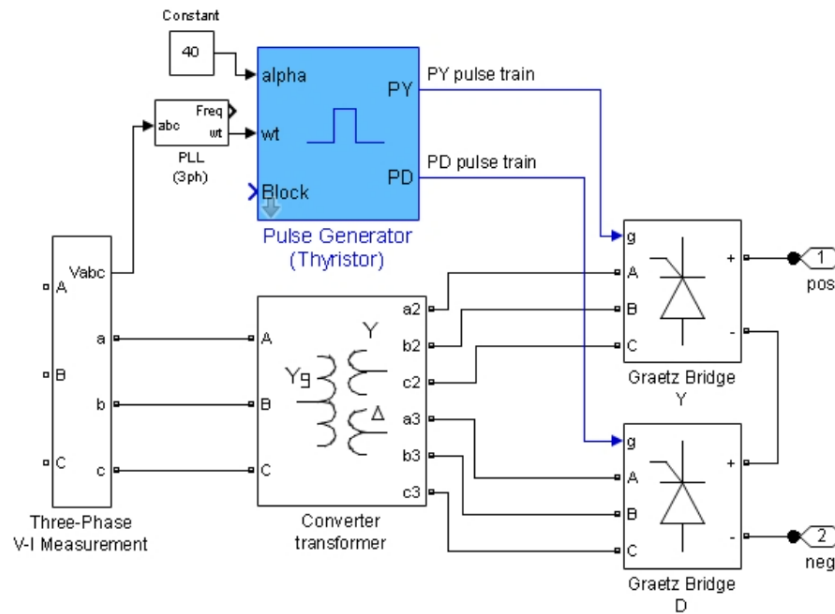


Figure 18. Control philosophy of 12-pulse rectifier unit (MathWorks, 2024a).

Voltage measurement from AC side is required to control the thyristor rectifier for synchronizing the pulses for each thyristor with the sine wave at power grid. Voltages are measured from the primary side of the rectifier transformers where the 15 degrees phase shift between the 12-pulse units is already existing. 30 degrees phase shift between the 6 pulse units shall be considered when forming pulses for both 6-pulse thyristor bridges. The firing angle is used to control voltage of the DC loop while the current is set as a constant current source.

5.6 IGBT rectifier model

IGBT rectifier topology is more complex compared to the thyristor topology due to power limitations of a single IGBT bridge. According to the power electronics supplier's budgetary quotation, the two IGBT units fed by a three winding transformer are connected in parallel and both units include three IGBT bridges. It is assumed that six pulse voltage source converters are used. The topology of the IGBT rectification system without control signals is presented in Figure 19.

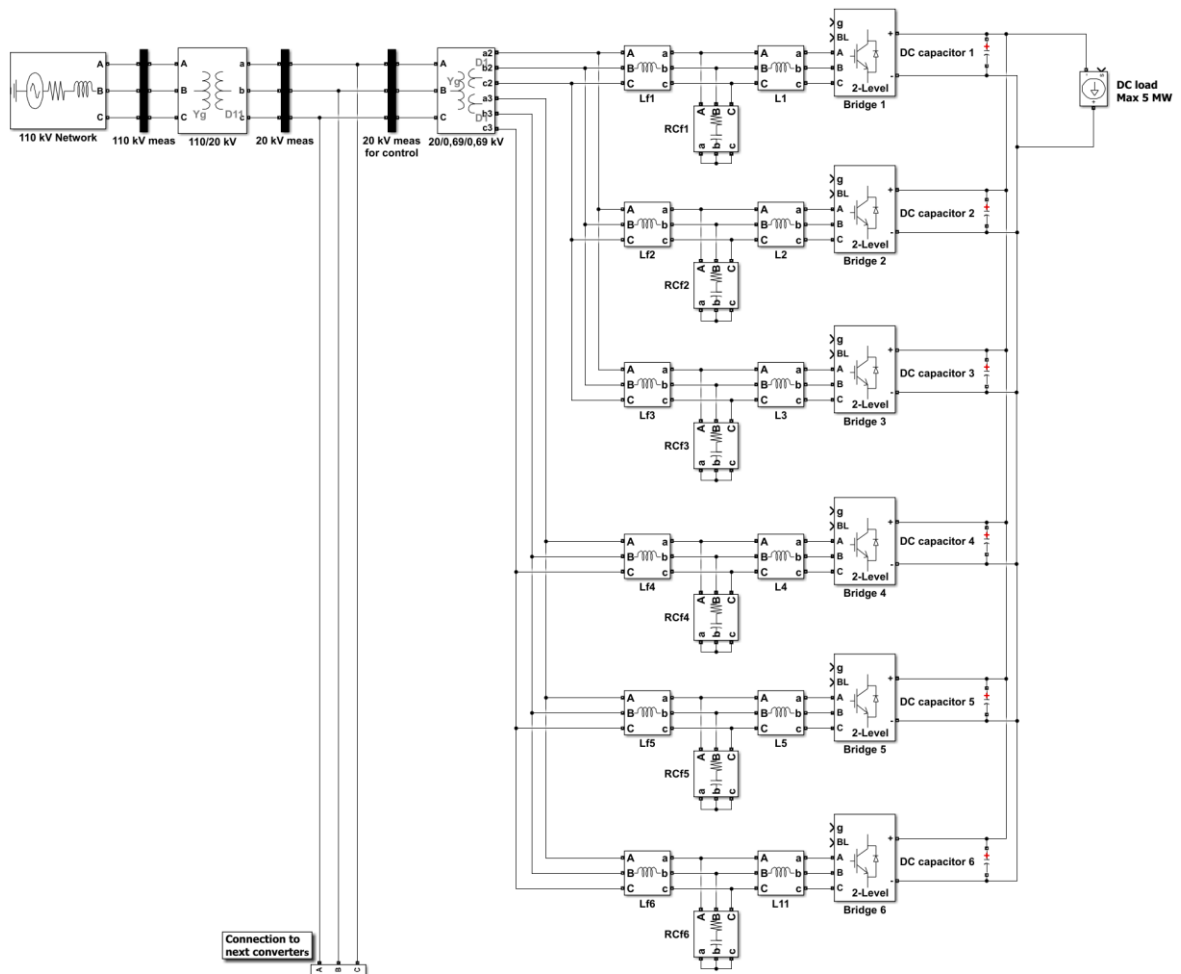


Figure 19. IGBT rectification system topology and power network. The figure presents a 5 MW DC load controlled by IGBT converter.

DC capacitors 12 mF at DC side are used after each IGBT bridge to stabilize the DC ripple. Circulating currents between the bridges can cause issues when utilizing parallel topology for the converter and capacitors together with the LCL filters can reduce possible circulating currents and stabilize the operation (Peltoniemi, 2024). Measuring points are connected on each level of the circuit to control and measure the operation of the IGBT converter. 10 pieces of IGBT rectifying units are connected parallel at the 20 kV voltage level to form the simulation model of a 50 MW electrolyser plant. The tapping's of the rectifier transformers are not needed to be utilized in this Simulink model.

5.6.1 LCL filter

The design of the LCL filter is based on a paper published by Liserre et al. 2005, which presents a step-by-step iterative procedure. One phase connection of an LCL filter can be seen from Figure 20, where damping resistor is not presented.

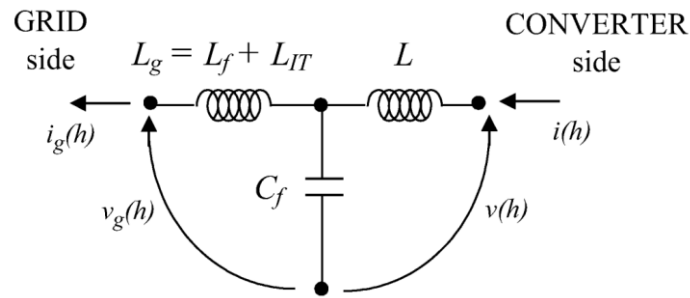


Figure 20. One phase connection of an LCL filter (Liserre et al. 2005).

The damping resistor R_f will be connected in the series with filter capacitor C_f . Sub-term g refers to the grid side of the filter and sub-term IT refers to isolation transformers which can be also called as rectifier transformer in this application.

Base values, impedance Z_b and capacitance C_b of the converter grid connection must be defined to calculate the filter parameters. Base impedance is defined according to equation 24 and base capacitance according to equation 25. (Liserre et al. 2005)

$$Z_b = \frac{U_{LL}^2}{P_n} \quad (24)$$

$$C_b = \frac{1}{\omega_n Z_b} \quad (25)$$

where P_n is rated active power of the converter and ω_n is angular frequency of the grid (Liserre et al. 2005).

Selection of the converter side inductance L is based on desired current ripple defined for the converter side. The grid side inductance L_g can be determined as a function of the converter side inductance L by using factor r . The grid side inductance L_g should also include

the grid inductance where the rectifier transformers secondary/tertiary coil inductances are considered in the thesis calculations. (Liserre et al. 2005)

The filter capacitor value C_f is defined as a function of the base capacitance C_b and factor x , where the factor x is percentual value of the power factor decrease desired at rated conditions (Liserre et al. 2005).

The factor r is based on calculation of ripple attenuation factor. Neglecting losses and filter damping, the attenuation can be defined according to equation 26. (Liserre et al. 2005)

$$\frac{i_g(h_{sw})}{i(h_{sw})} = \frac{1}{|1+r(1-ax)|} \quad (26)$$

where $i_g(h_{sw})$ is the grid side harmonic current at switching frequency, $i(h_{sw})$ is the converter side harmonic current at the switching frequency and a is a constant defined by equation 27 (Liserre et al. 2005).

$$a = LC_b\omega_{sw}^2 \quad (27)$$

where ω_{sw} is angular frequency of switching frequency (Liserre et al. 2005).

The resonant frequency f_{res} can be calculated using equation 29, where the resonant angular frequency ω_{res} is first calculated by using equation 28 (Liserre et al. 2005).

$$\omega_{res} = \sqrt{\frac{L+L_g}{LL_gC_f}} \quad (28)$$

$$f_{res} = \frac{\omega_{res}}{2\pi} \quad (29)$$

The filter requires also damping which is implemented by using a resistor in series with the filter capacitor. Impedance value of the filter capacitor at the resonant frequency is selected for damping resistance according to equation 30. (Liserre et al. 2005)

$$R_f = \frac{1}{2\pi f_{res}C_f} \quad (30)$$

According to the Liserre et al. procedure, there are certain limitations what affects the iteration process to find the filter parameters. Next limitations are considered during the process:

- The factor x is limited by the maximum decrease of power factor at the rated load where the limitation is maximum 5%

- The total value of filter inductance is limited by maximum 10% reactance from the base impedance to limit the voltage drop at AC side
- The value of resonant frequency shall be at least 10 times the grid frequency, but maximum 50% of the switching frequency to avoid resonance issues
- The passive damping resistor cannot affect too high losses for the application where a maximum of 1% of the rated power can be used as a baseline. (Liserre et al. 2005)

Experimental tests indicated that it was beneficial to add high inductance to the converter side in relation to grid side and use the maximum capacitor value to have a good performance for the filter and fulfill the limitations given above. There are six filters in the setup, where the nominal power is also evenly distributed because of the common DC loop. Parameters defined for the LCL filters are presented in Table 13.

Table 13. Parameters for LCL filters utilized in the Simulink model

Quantity	Value
Converter side inductance L	347.22 μH
Grid side inductance L_f	0.83 μH
Capacitance C_f	0.83 μF
Damping resistance R_f	9.33 $\text{m}\Omega$

5.6.2 Control of the IGBT rectifier

Modulation of the IGBT rectifier used in the Simulink model is based on the SPWM method presented in chapter 4.2.1. The input signal V_{MOD} required for SPWM modulation is generated by several control circuits that use AC side phase currents and voltages, as well as the DC link voltage. In commercial solutions, AC side currents and voltages are typically measured from the low-voltage side of the rectifier transformers for control purposes (Peltoniemi, 2024). However, in this research, the measurement point was selected on the MV side of the transformer. This selection was made to simplify the model, where unity power factor is

desired in the 20 kV grid without separate reactive power offset control circuits. A phase shift over the rectifier transformer must be considered in the measurement loop to synchronize the PWM signal with voltage phasing at the low voltage side. Also, the performance of the Simulink model becomes too heavy, if separate controls are used for the each 6-pulse IGBT unit. Location of the control measurement is shown in the Figure 19.

AC voltage and current measurements from the three-phase system are transferred into dq0 reference frames (direct, quadrature, zero) by using Park transformation, as presented in Figure 21 (Giroux et al. 2022).

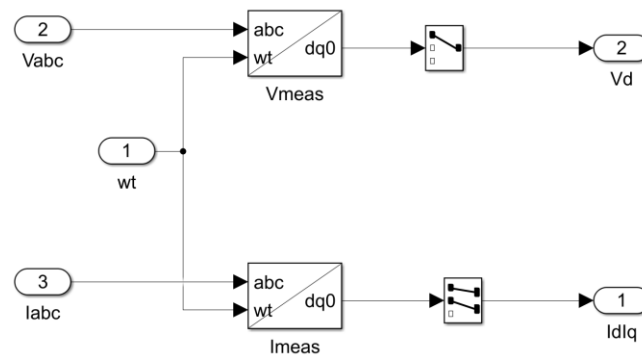


Figure 21. AC voltage and current measurements transferred to dq0 reference frame by using Park transformation (Giroux et al. 2022).

The time-domain three phase (abc) reference frame components are transferred to the dq0 components in a rotating reference frame, where ω defines rotational speed of the dq0 reference frame (MathWorks, 2024b). Control loops are in the dq reference frame because the numerical values without time-domain are easier to manage in control loops. Measurements are transferred to per-unit mode before the Park transformation. Selectors at dq0 reference frame signals are used to select only needed signals for further processing, which are V_d , I_d and I_q .

DC voltage needs to be adjusted by rectifier which requires separated control loop. DC voltage regulator is presented in Figure 22.

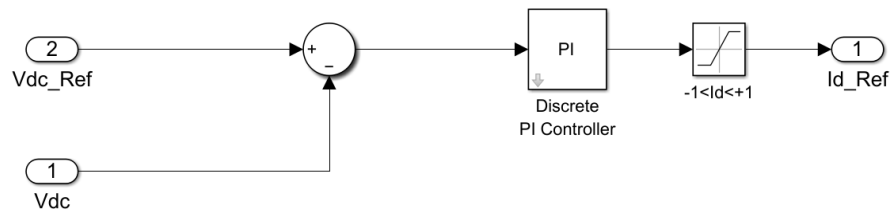


Figure 22. DC controller, where the controller output gives reference for the current I_d (Giroux et al. 2022).

The DC voltage regulator gives reference to the separated I_d current controller. When the current I_d is positive, the converter is absorbing active power. The current component I_q affects reactive power, so the I_q reference is set to constant zero, because unity power factor is desired in the model. (Giroux et al. 2022). The current control loop is presented in Figure 23.

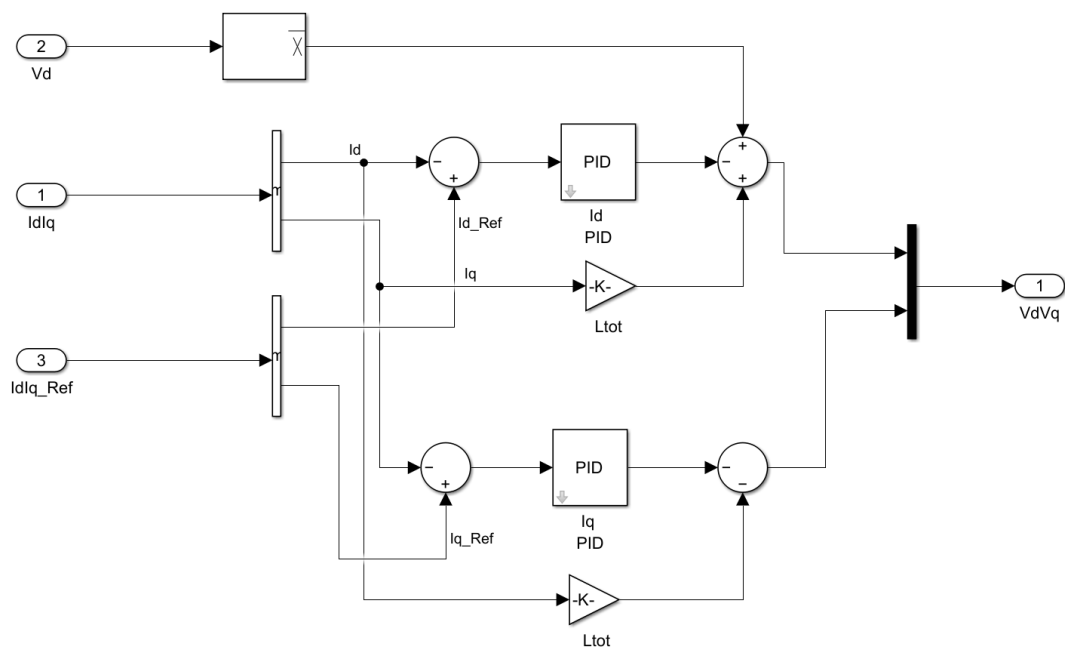


Figure 23. Decoupled current controllers with feed-forward properties (Giroux et al. 2022).

The I_d and I_q current controllers are decoupled, but the current of the other component multiplied by inductance on the AC side is used for feed-forward control to prevent a mutual

interference in the control loop (Liao et al. 2000). The current control results V_d and V_q components, what are used as references for PWM generators.

The V_d and V_q signals from the dq0 reference rotating frame need to be transferred back to the three-phase (abc) signals for PWM generators, by using the inverse Park transformation. The three-phase signal $V_{MOD} = U_{ref}$ is then used together with carrier signal V_{TRIANG} to generate pulses for the IGBT transistors, as already described in chapter 4.2.1. (Giroux et al. 2022) The carrier waveforms are generated internally in the PWM generators and switching frequency in the model is selected 3.6 kHz, which corresponds the commercial converter operation. Connection of PWM generators is presented in Figure 24.

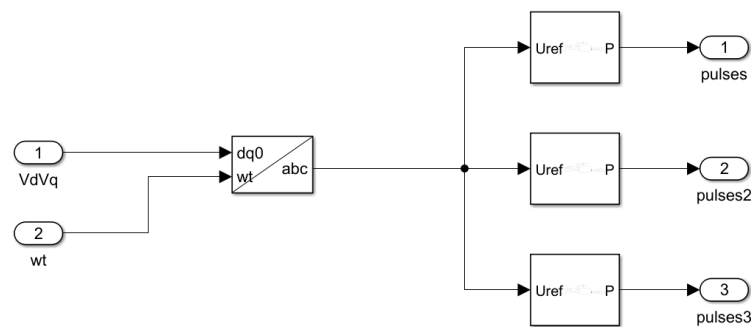


Figure 24. Inverse Park transformation and PWM generators (Giroux et al. 2022).

Controls of the IGBT bridges are divided in three segments. The first PWM generator is controlling bridges 1 and 4, the second generator is controlling bridges 2 and 5, and the third generator set is controlling bridges 3 and 6. Carrier waveforms are shifted 2.09 degrees between the PWM generators according to equation 17.

5.7 Simulation results

Simulations were done to compare the thyristor and IGBT controlled rectifiers in a setup with multiple converters in the same grid, to understand how different load scenarios effect the power quality. Proposed operation scenarios are presented in Table 14.

Table 14. Load scenarios where one unit means one 5 MW electrolyser

Scenario number	Load scenario for total DC power	Total DC power
1	100% load	50 MW
2	60% load, all units are equally loaded	30 MW
3	20% load, all units are equally loaded	10 MW
4	60% load implemented with four units in standby and six units at 100%	30 MW
5	20% load implemented with eight units in standby and two units at 100%	10 MW
6	90% load where one 5 MW unit in standby and all other units are fully loaded (only thyristor model tested)	45 MW

In normal operation, all consumers are expected to be in operation and equally loaded. Partial load scenarios are also investigated in a way, where part of the electrolysers is in standby. Maintenance of the electrolyser plant is also required. For example, overhauling after a certain operating period, when electrolyser stacks need to be replaced or maintained. This means that at least one of the 5 MW units will be out of operation. Scenario number 6 is interesting for the thyristor control, because the 24-pulse topology will be lost if both 12-pulse units are not equally loaded.

Simulation results were compared to relevant standards at the 20 kV and 110 kV voltage levels to verify the power quality against the standards. In addition to DC power, the total active power, apparent power and reactive power are reported in each voltage level. Short circuit current in the network is used as initial data for selection of limit values in the IEEE 519-2022 standard according to chapter 2.1.2. The lowest IEEE 519-2022 standard values are utilized as limit values at the 20 kV voltage level study and second highest standard values are utilized at the 110 kV voltage study.

Both THD, TDD and individual harmonics conditions are used as limits to indicate compliance with relevant standards. Utilized harmonic content ranges h_n for each calculation and conditions are informed in defined column of result tables. $TDDi$ calculation is made according to equation 31.

$$TDDi = \sqrt{\sum_2^{\max} \left(\frac{i_h}{i_L}\right)^2} \quad (31)$$

where i_L is the maximum demand load current. The fundamental amplitude at 100% load is utilized as the maximum demand load current for the $TDDi$ calculation when studying compliance with IEEE 519-2022 standard. The active power current at 100% load is utilized as i_L when studying compliance with Fingrid's 110 kV grid report. THD calculation is made according to equation 32.

$$THD = \sqrt{\sum_2^{\max} \left(\frac{i_h \text{ or } u_h}{i_1 \text{ or } u_1} \right)^2} \quad (32)$$

where voltage or current harmonics content is a percentual part of the fundamental amplitude.

5.7.1 Results of thyristor rectifier simulations

Table 15 presents the results of harmonic currents compared to the IEEE 519-2022 standard limits in both 20 kV and 110 kV voltage levels.

Table 15. Current distortion results for thyristor model compared to the IEEE 519-2022 standard. Green color values are within the standard recommendations, red color values do not meet the standard recommendations and clear color values are informative

Scenario	DC Power [MW]	Firing angle [°]	20 kV	20 kV IEEE 519-2022 recommendations			110 kV	110 kV IEEE 519-2022 recommendations		
			$THDi$	i_{h2-50} [%]	$TDDi_{h2-50}$ [%]	Individ. i_{h2-50}	$THDi$	i_{h2-50} [%]	$TDDi_{h2-50}$ [%]	Individ. i_{h2-50}
1	50.06	10.0	2.07	2.07	x	2.06	2.06	x		
2	30.05	21.5	4.79	3.00	x	4.77	3.00	x		
3	10.12	34.0	5.80	1.35	x	5.74	1.34	x		
4	30.04	13.0	2.81	1.68	x	2.80	1.68	x		
5	10.06	15.0	3.39	0.68	✓	3.36	0.68	✓		
6	45.22	10.0	2.32	2.09	x	2.32	2.09	x		

The $TDDi$ of harmonic currents are within the standard limit in each scenario, but the individual harmonic content is above the standard level excluding scenario 5. The $THDi$ level

has increased due to the increased firing angle, but because the $TDDi$ is studied in the IEEE 519-2022 standard, the largest relative value is found in scenario 2. Based on simulation, partial loads are beneficial to operate in a way where part of the electrolyzers are on standby, when considering only harmonic distortion. The reason for this is the lower firing angle for those in operational rectifier units. Figure 25 presents a chart where current distortion is compared to the IEEE 519-2022 recommendations at 20 kV voltage level where crossing of the individual harmonics can be observed at 100% load.

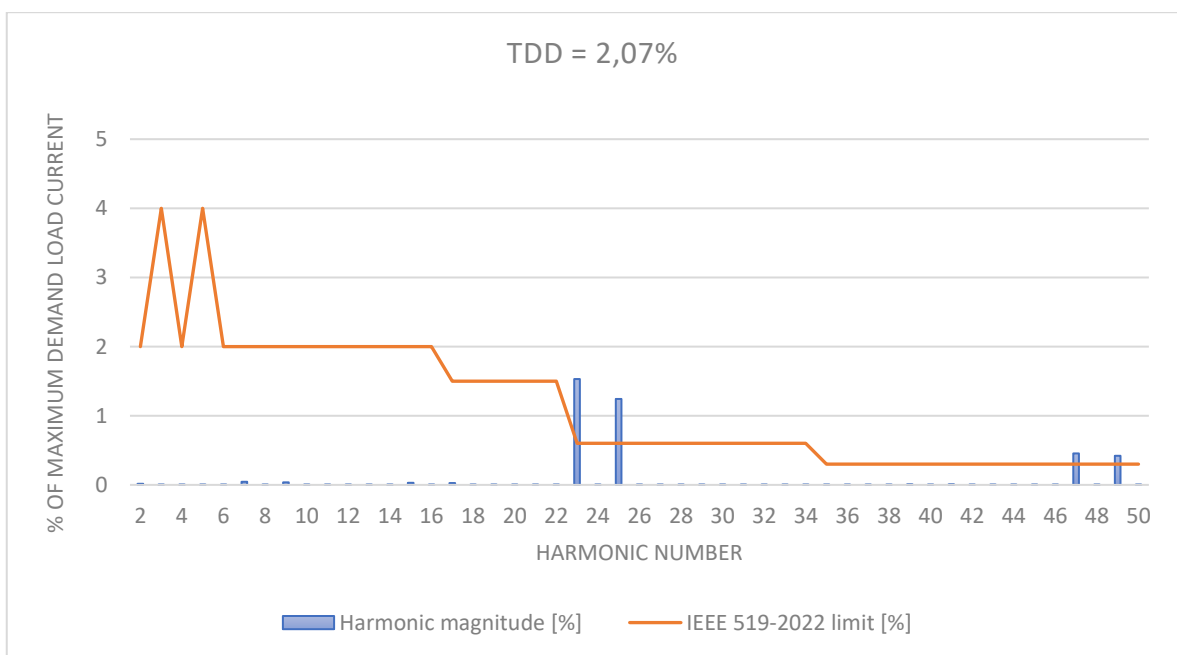


Figure 25. Scenario 1, current distortion, thyristor 24-pulse rectifiers at 100% load, PCC 20 kV.

The highest crossings occurs by order 23rd and 25th harmonics which are the top harmonics, when using the 24-pulse rectifier. Also, 47th and 49th harmonic currents are above the standard IEEE 519-2022 limit. Lower than the order number 23 harmonics are on insignificant level, when operating the 24-pulse rectifying system.

As a comparative study, it's relevant to see the current distortion of scenario 1 at the 110 kV voltage level as well. Figure 26 presents the harmonic currents compared to the IEEE 519-2022 standard at the 110 kV voltage step at 100% load.

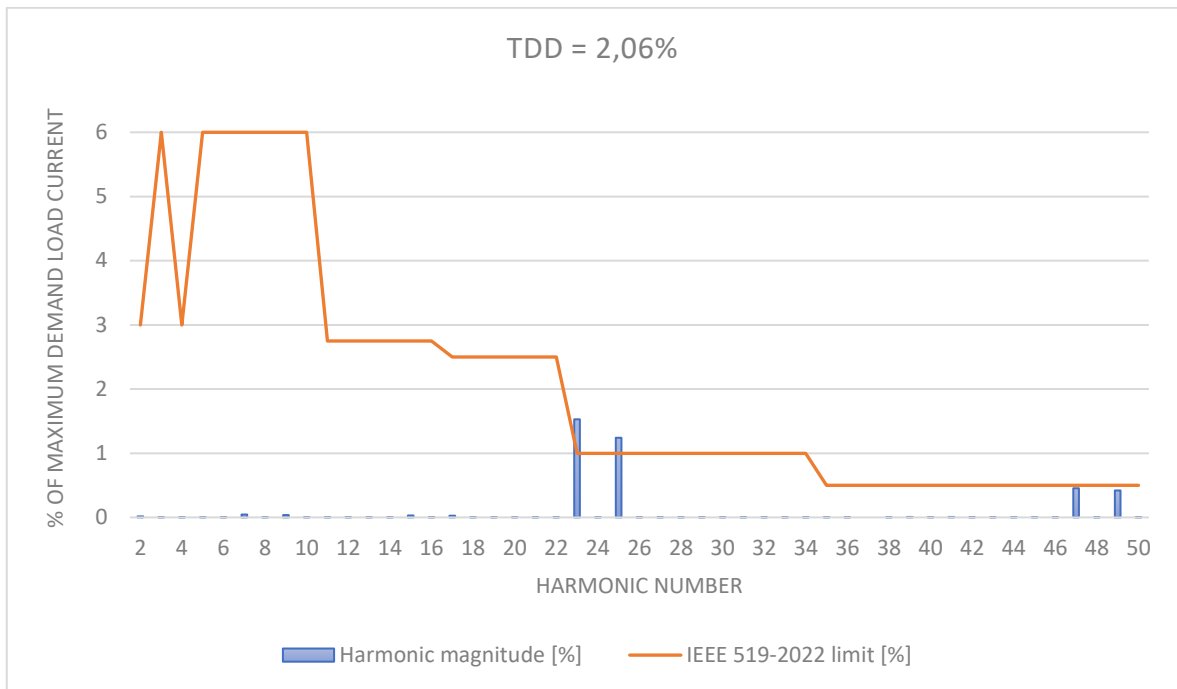


Figure 26. Scenario 1, current distortion, thyristor 24-pulse rectifiers at 100% load, PCC 110 kV.

The main transformers characteristics affect current distortion, and standard limits differ at 110 kV voltage level. Harmonic orders 47 and 49 fall below the standard limit but the 23rd and 25th harmonic currents remain above the standard limit and recommendations of the standard IEEE 519-2022 have not met, when studying the individual harmonics.

The scenario number 6 simulates an exceptional situation, where one 5 MW unit is on standby and causing malfunction in one 24-pulse system. Harmonic distortion spectrum for the scenario 6 is presented in Figure 27.

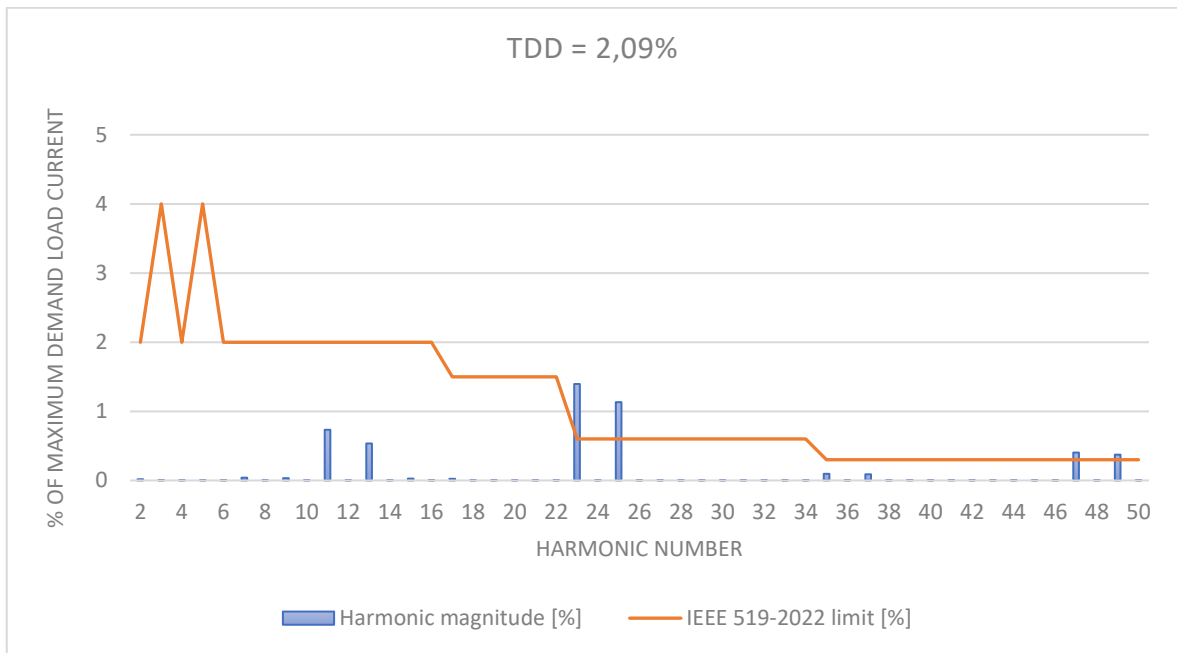


Figure 27. Scenario 6, current distortion, thyristor 24-pulse rectifiers and one 12-pulse rectifier at total 90% load, PCC 20 kV.

Based on Figure 27, harmonic currents of orders 11, 13, 35, and 37 are present because of the one 5 MW unit is operating as a 12-pulse system due to loss of the intended 24-pulse pair. Those harmonic currents are within the standard limits and crossing the standard limit happens still by order $24n \pm 1$ harmonic currents.

The IEEE 519-2022 includes also recommendations for the voltage distortion limits which were studied in both voltage levels. Results of harmonic voltages compared to the IEEE 519-2022 standard are presented in Table 16.

Table 16. Voltage distortion results for thyristor model compared to the IEEE 519-2022 standard. Green color values are within the standard recommendations, red color values do not meet the standard recommendations and clear color values are informative

Scenario	DC Power [MW]	Firing angle [°]	20 kV IEEE 519-2022 recommendations		110 kV IEEE 519-2022 recommendations	
			$THDu_{h2-50}$ [%]	Individ. u_{h2-50}	$THDu_{h2-50}$ [%]	Individ. u_{h2-50}
1	50.06	10.0	4.65	✓	0.44	✓
2	30.05	21.5	6.48	x	0.62	✓
3	10.12	34.0	3.40	✓	0.33	✓
4	30.04	13.0	3.53	✓	0.34	✓
5	10.06	15.0	1.35	✓	0.13	✓
6	45.22	10.0	4.32	✓	0.41	✓

Voltage harmonics performed better compared to the harmonics current study and only scenario number 2 couldn't reach the limits of standard at the 20 kV voltage level. Both $THDu$ and individual voltage harmonics are out of the IEEE 519-2022 recommendations at the scenario number 2. The 23rd and 25th harmonic voltages exceed the IEEE 519-2022 limits, and the $THDu$ limit of 5% is also exceeded. The spectrum of harmonic voltages at scenario number 2 is presented in Figure 28 and crossing the standard limits can be observed.

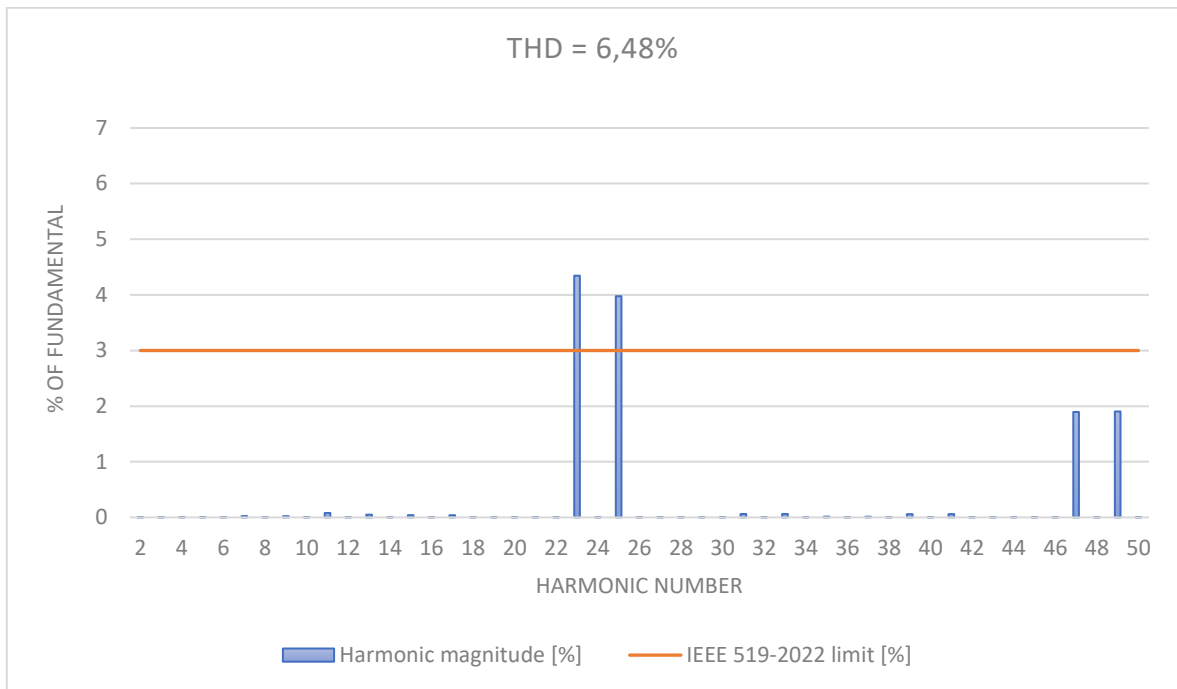


Figure 28. Scenario 2, voltage distortion, thyristor 24-pulse rectifiers at total 60% load, PCC 20 kV.

Fingrid's 110 kV grid requirements include limits for both current and voltage distortion. Table 17 presents the results of harmonic distortion compared to Fingrid's 110 kV requirements and the SFS-EN 50160:2022 110 kV recommendations.

Table 17. Current and voltage distortion for thyristor model compared to Power quality in Fingrid's 110 kV grid report and 110 kV SFS-EN 50160:2022 standard. Green color values are within the requirements, red color values do not meet the requirements and clear color values are informative

Scenario	DC Power [MW]	Firing angle [°]	110 kV Fingrid's requirements				SFS-EN 50160:2022 110 kV recommendations
			$TDDi_{h2-100}$ [%]	I_p [A]	$THDu_{h2-50}$ [%]	Individ. u_{h2-50}	Individual u_{h2-24}
1	50.06	10.0	2.22	5.86	0.44	✓	✓
2	30.05	21.5	3.22	8.59	0.62	✓	✓
3	10.12	34.0	1.51	3.75	0.33	✓	✓
4	30.04	13.0	1.81	4.84	0.34	✓	✓
5	10.06	15.0	0.73	1.97	0.13	✓	✓
6	45.22	10.0	2.25	5.71	0.41	✓	✓

Based on the simulations, the TDDi values are within the required level in all scenarios but the psophometric value of phase current is above the limit at the scenarios 1, 2 and 6. Based on this study, can be also stated that it's beneficial to operate the partial power scenarios in a way where part of the electrolyzers are on standby when considering the harmonic distortion. Voltage distortions can be found to be following Fingrid's requirements and also within the SFS-EN 50160:2022 standard recommendations.

Powers were also investigated in the Simulink model for both 20 kV and 110 kV voltage steps. The results for power study can be found in Table 18 for the 20 kV voltage step and in Table 19 for the 110 kV voltage step.

Table 18. Power information of thyristor model at the 20 kV voltage step

Scenario	DC Power [MW]	Firing angle [°]	20 kV network			
			Apparent power [MVA]	Active power [MW]	Reactive power [MVA _r]	<i>PF</i>
1	50.06	10.0	53.30	51.09	14.9	0.96
2	30.05	21.5	33.63	30.51	13.88	0.91
3	10.12	34.0	12.58	10.27	7.21	0.82
4	30.04	13.0	32.33	30.66	10.14	0.95
5	10.06	15.0	10.91	10.27	3.66	0.94
6	45.22	10.0	48.12	46.15	13.41	0.96

Table 19. Power information of thyristor model at the 110 kV voltage step

Scenario	DC Power [MW]	Firing angle [°]	110 kV network			
			Apparent power [MVA]	Active power [MW]	Reactive power [MVA _r]	<i>PF</i>
1	50.06	10.0	54.65	51.18	19.14	0.94
2	30.05	21.5	34.38	30.56	15.66	0.89
3	10.12	34.0	12.83	10.30	7.62	0.80
4	30.04	13.0	32.91	30.71	11.79	0.93
5	10.06	15.0	11.06	10.29	4.02	0.93
6	45.22	10.0	49.22	46.22	16.89	0.94

Increasing the firing angle results in higher reactive power and the reactive power is not compensated in the model. The lowest power factor occurs in scenario 3, but the actual MVA_r value is low due to the low power level in the scenario. The highest power factors occur in scenarios with the lowest firing angle. The resistance and inductance of the main transformers affect the higher active and reactive powers on the 110 kV side of the network compared to the 20 kV values. According to Helen Sähköverkko's definition described in chapter 2.4, the power factor does not need to be 1 to avoid reactive power fees. If a customer-specific free part is not considered, the reactive power fee should be paid starting from 11.25 MVA_r at full 100% operation, unless the reactive power is compensated by external equipment. To avoid reactive power payments, the power factor should be 0.99. As shown

in the results, the minimum firing angle is 10 degrees, which leaves possibilities for better optimization of voltage control

5.7.2 Results of IGBT rectifier simulations

Table 20 presents the results of harmonic currents for the IGBT rectifier model compared to the IEEE 519-2022 standard at both 20 kV and 110 kV voltage levels.

Table 20. Current distortion results for IGBT model compared to the IEEE 519-2022 standard. Green color values are within the standard recommendations and clear color values are informative

Scenario	DC Power [MW]	20 kV	20 kV IEEE 519-2022 recommendations		110 kV	110 kV IEEE 519-2022 recommendations	
		THDi	i_{h2-50} [%]	$TDDi_{h2-50}$ [%]	Individ. i_{h2-50}	THDi	i_{h2-50} [%]
1	50.12	2.65	2.65	✓	2.51	2.51	✓
2	30.02	2.47	1.45	✓	2.84	1.72	✓
3	10.07	6.08	1.30	✓	6.89	1.39	✓
4	30.08	2.34	1.40	✓	2.28	1.38	✓
5	10.03	2.11	0.42	✓	2.02	0.41	✓

All studies for the IGBT rectifier models fall below the limit values of the standard IEEE 519-2022 recommendations. The $THDi$ level is highest at the scenario number 3, where all units are in operation at 20% load, but the relative value $TDDi$ is far from the standard limitation. Individual harmonics are also below the limit values of standard recommendations. At the partial load scenarios, where all units are loaded equally the harmonic current levels are slightly higher at the 110 kV side of the network, which differs from the thyristor model. Based on the simulation results, the low power loading scenario is beneficial to operate in a way where part of the electrolyzers is on standby. Figure 29 presents the spectrum of harmonic currents for the IGBT rectifiers at 100% load at the 20 kV voltage level and comparison to limit values for the IEEE 519-2022 standard.

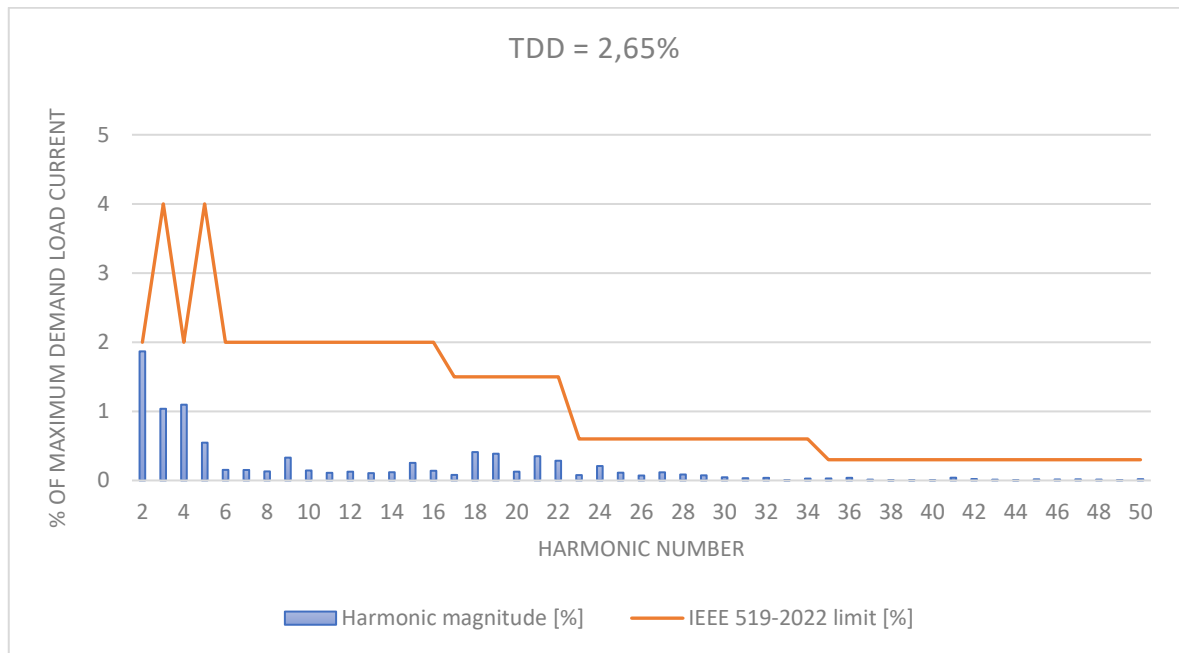


Figure 29. Scenario 1, current distortion, IGBT rectifiers at 100% load, PCC 20 kV.

Spectrum of the harmonic content at IGBT operation differs from the thyristor operation. Harmonic content exists mostly at the lower frequencies and is settled for higher frequencies except the frequencies near the switching frequency, which is not visible in Figure 29. The standard IEEE 519-2022 considers only harmonics up to order 50.

Voltage distortion is examined also for the IGBT rectifier model where all scenarios fulfill the recommendations of the IEEE 519-2022 standard. The results of the study of harmonic voltages are presented in Table 21.

Table 21. Voltage distortion results for the IGBT model compared to the IEEE 519-2022 standard. Green color values are within the standard recommendations and clear color values are informative

Scenario	DC Power [MW]	20 kV IEEE 519-2022 recommendations		110 kV IEEE 519-2022 recommendations	
		$THDu_{h2-50}$ [%]	Individ. u_{h2-50}	$THDu_{h2-50}$ [%]	Individ. u_{h2-50}
1	50.12	1.47	✓	0.16	✓
2	30.02	1.38	✓	0.15	✓
3	10.07	1.17	✓	0.12	✓
4	30.08	0.90	✓	0.09	✓
5	10.03	0.38	✓	0.04	✓

The highest $THDu$ level has been found from the scenario number 1. The $THDu$ levels are lower at the 110 kV side of the power network due to the impedance characteristics of the network. The spectrum of individual harmonic voltages at the 20 kV voltage level is presented in Figure 30.

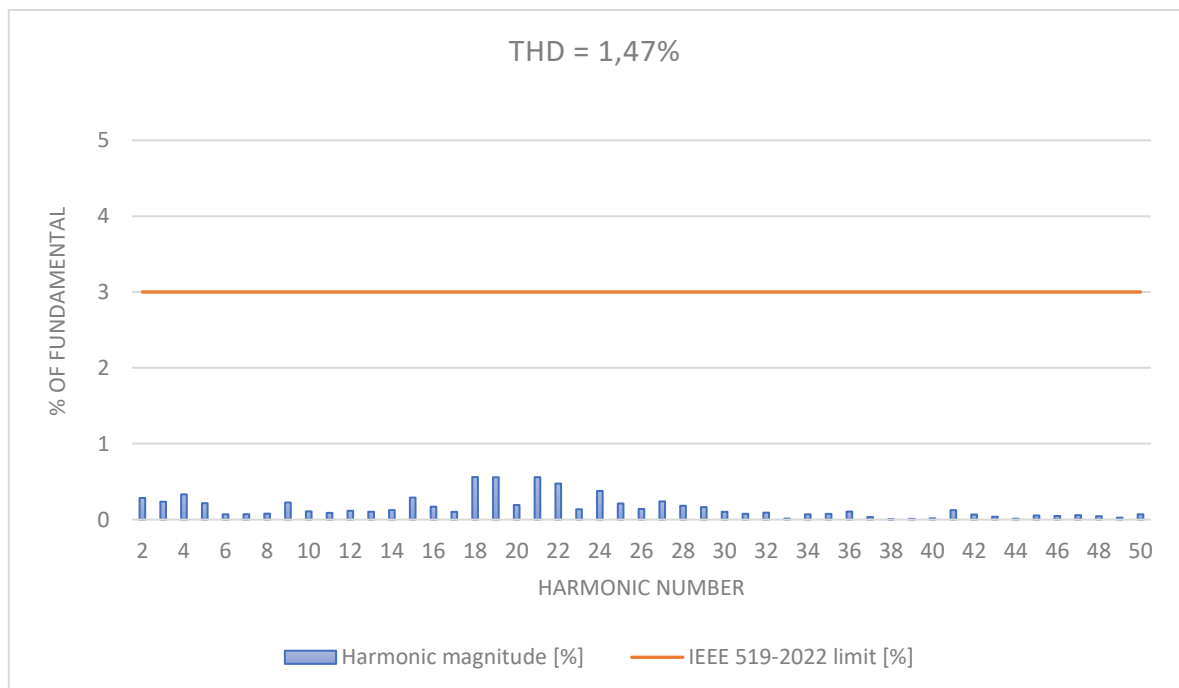


Figure 30. Scenario 1, voltage distortion, IGBT rectifiers at total 100% load, PCC 20 kV.

The voltage distortion spectrum at scenario number 1, which is reviewed at the 20 kV voltage level, appears to have a slightly different shape compared to the harmonic current study. Low-frequency harmonics are not dominant, but the highest harmonic content appears in the range from order 18 to 24 harmonic voltages. Harmonic voltage levels fall far below the IEEE 519-2022 standard recommendation limits.

All scenarios studied fulfill also the Fingrid's 110 kV requirements and the SFS-EN 50160:2022 standard recommendations. The results of harmonic distortion study compared to Fingrid's 110 kV requirements and SFS-EN 50160:2022 standard recommendations are presented in Table 22.

Table 22. Current and voltage distortion for the IGBT model compared to the Power quality in Fingrid's 110 kV grid report and 110 kV SFS-EN 50160:2022 standard. Green color values are within the requirements and clear color values are informative

Scenario	DC Power [MW]	110 kV Fingrid's requirements				SFS-EN 50160:2022 110 kV recommendations
		$TDDi_{h2-100}$ [%]	I_p [A]	$THDu_{h2-50}$ [%]	Individ. u_{h2-50}	Individual u_{h2-24}
1	50.12	2.50	2.94	0.16	✓	✓
2	30.02	1.74	2.97	0.15	✓	✓
3	10.07	1.45	2.35	0.12	✓	✓
4	30.08	1.40	1.74	0.09	✓	✓
5	10.03	0.44	0.69	0.04	✓	✓

The study against Fingrid's harmonic currents limitations is concluded up to order 100th harmonics. The 3.5 kHz switching frequency is observable when reviewing the individual harmonic currents even though the LCL filters are used in the rectifier topology. The amplitude of the individual harmonic currents does not cause exceeding of the $TDDi$ or psophometric value of phase current above the Fingrid's requirements.

Results of power study at the 20 kV voltage step can be seen from Table 23 and at the 110 kV voltage step from Table 24.

Table 23. Power information of IGBT model at the 20 kV voltage step

Scenario	DC Power [MW]	20 kV network			
		Apparent power [MVA]	Active power [MW]	Reactive power [MVA _r]	<i>PF</i>
1	50.12	51.12	51.12	0.00	1.00
2	30.02	30.84	30.84	0.00	1.00
3	10.07	10.68	10.68	0.00	1.00
4	30.08	30.84	30.84	0.00	1.00
5	10.03	10.24	10.24	0.00	1.00

Table 24. Power information of IGBT model at the 110 kV voltage step

Scenario	DC Power [MW]	110 kV network			
		Apparent power [MVA]	Active power [MW]	Reactive power [MVA _r]	<i>PF</i>
1	50.12	51.33	51.18	3.75	0.997
2	30.02	30.92	30.87	1.47	0.998
3	10.07	10.70	10.68	0.33	0.997
4	30.08	30.91	30.87	1.49	0.998
5	10.03	10.27	10.26	0.34	0.999

The power factor at the 20 kV voltage level can be maintained at 1.00 due to the power factor control capability of the IGBT rectifying units. The main transformers inductance is consuming reactive power and is the reason why power factor is below 1 at the 110 kV voltage level, and the power factor is controlled at the 20 kV voltage step in Simulink model. The reactive power level is dependent on the plant operational power since the reactive power is consumed only in the main transformer's inductance and the consumed reactive power doesn't cause separated reactive power payments described in chapter 2.4. The measured 100% load apparent power is 3.32 MVA lower compared to similar scenario with the thyristor model, which can be noted when dimensioning the power distribution components.

5.8 Verification of simulation results

The simulation models are based on given components, topologies and parameters reported. Functionality of the Simulink models and results can be compared to the theory part presented in chapter 4 and the results can also be compared with existing research.

Control of the thyristor rectifier can be stated to be following the theory part, where the firing angle is used as control variable. Increased firing angle is reducing output power of the converter but results also lower PF and higher harmonic distortion towards the power grid. The 24-pulse operation can be discovered from harmonic spectrums presented in this chapter, where the highest harmonic frequencies are following the Fourier series presented in equation 15.

The IGBT converter has been controlled by amplitude and phase shift of the reference signal, what is generated by utilizing several control loops. The output power can be controlled as planned and PF can be kept unity on the 20 kV voltage level, where the control measurements are located. The LCL filter is reducing harmonic currents near the switching frequency and requirements of the Fingrid's report are fulfilled, where these frequencies are present into the investigated range. Phase shifts between the carrier waveforms are implemented according to equation 17, which has been found beneficial based on experimental tests.

The IGBT technology has been found to perform better in power quality compared to the thyristor technology. The founding follows other studies on a large scale, but findings related to the THDi levels don't correspond with most of the previous studies. According to the simulation results, the THDi level of thyristor model is slightly lower at 100% load compared to the IGBT model. However, the simulation models are based on the large-scale plant, where multiple rectifiers are parallel connected, and the environment and parameters do not correspond fully with other studies.

Specific items may cause inaccuracy for the simulation results compared to the commercial converters. The DC loop does not have the real characteristics of the PEM electrolyser but is simulated as a DC load, what is not corresponding fully with the realistic application. Transformer parameters approximated are based on nameplate values, where the inductance and resistance values are assumed to be split equally for both sides of the transformer. Inductance and resistance of the transformers affect characteristics of the entire distribution

grid. Effects of magnetization inductance have been found to be nonexistent for power quality, if high enough value has been used in the simulation models. Electrical values of thyristor and IGBT components are based on Simulink's default values, where the real values from power electronics suppliers were not available. Electrical values of components are affecting the switching characteristics and therefore can affect power quality as well. Dimensioning of the LCL filter in IGBT model has an effect for harmonic distortion and optimization of the filter parameters could be improved. Control of the IGBT rectifiers is based on several different control loops, where multiple parameters are affecting the functional totality. Parameters together with selected modulation method are affecting the performance of rectification models.

Voltage and current waveforms of rectifier operations are presented in Appendices 2-5. All measurements related to power quality and reactive power have been measured from the simulation period 0.4-0.5 seconds, where the operation has been stabilized.

6 Distribution of CAPEX costs

One result of this research is understanding the division of CAPEX costs between the technologies. Budgetary quotation received from power electronics supplier can be used to evaluate the cost division where the simulation results will support and give also other observations of the project CAPEX costs distribution. Currency values are not specified in the thesis, because the initial data is based on a single supplier and prices are not public information. The following items are considered in the comparison of CAPEX costs division:

- Rectifier equipment (including passive filters)
- Rectifier transformers
- Reactive power compensation unit
- CAPEX difference of electricity connection to power grid

Distribution of CAPEX costs between technologies is presented in Figure 31.

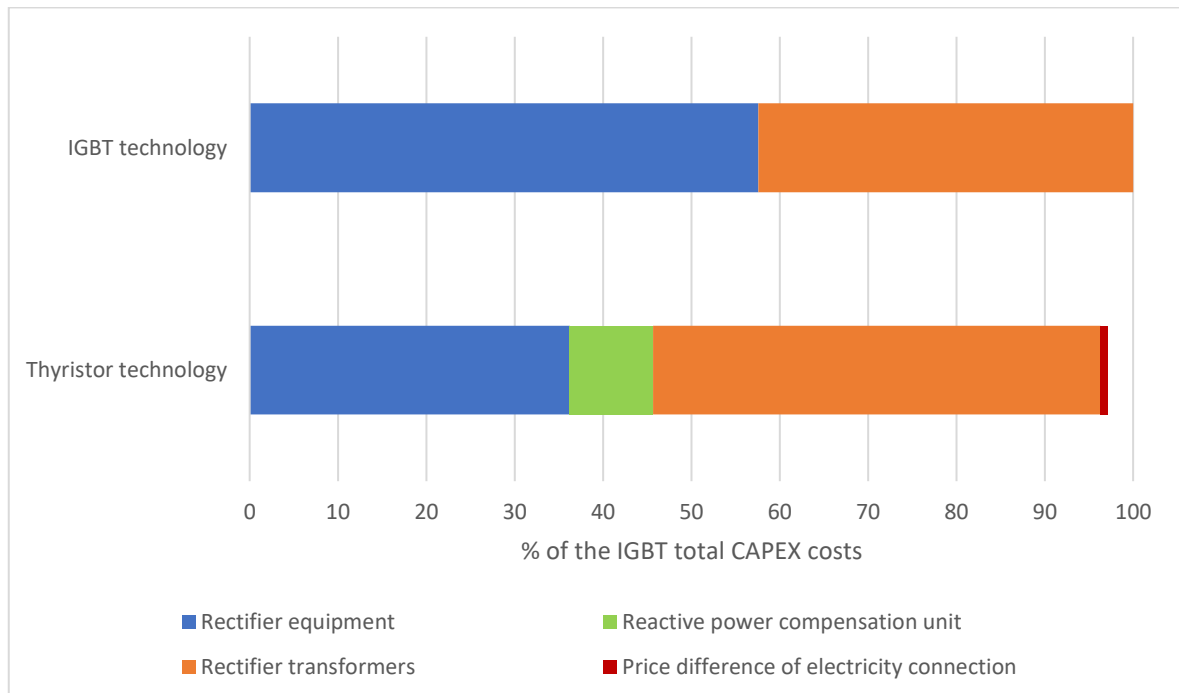


Figure 31. CAPEX cost distribution between the technologies in relation to total cost of the IGBT technology. Possible electricity filtering costs are excluded.

The IGBT technology costs consist of rectifier equipment costs and rectifier transformer costs while the thyristor technology costs include also the reactive power compensation unit and a higher price for the electricity connection. The IGBT technology is more expensive in power electronics, but the technology does not require a special type of transformer, which appears to be lower cost than the requirements of thyristor technology. The thyristor technology requires a three winding transformer with 30 degrees phase shift and delta-wye connection difference at secondary side, which increases the costs. While the IGBT technology has the capability to control reactive power, the thyristor technology requires an external reactive power compensation unit. Total costs of thyristor converters and external reactive power compensation are still lower than IGBT technology costs. Electricity connection is dimensioned according to apparent power, what also includes reactive power consumption. Because the thyristor technology cannot operate naturally at the unity power factor, possible defects of external compensation equipment shall be considered and there's why the electricity connection shall be bigger compared to the IGBT technology. The cost of a bigger electricity connection is considered in the distribution of CAPEX costs, which plays a minor role. (Helen Sähköverkko, 2025) Additionally, it should be noted that the higher apparent power affects other dimensioning as well, as for example the main transformer, switchgears, cables, busbars etc. and these costs are not considered in the presented CAPEX costs distribution.

Based on the modelling, the power quality of thyristor rectifying equipment does not comply with the requirements of the utilized standards and grid code in all modelled scenarios. Planned actions and possible external filtering unit against the harmonic distortion shall be considered, what might increase the CAPEX costs as well. These actions are not considered in the presented CAPEX costs distribution.

The results of CAPEX costs distribution are based on budgetary quotation received from a single supplier, which may cause inaccuracy for the results, since the pricing of technologies may vary depending on the supplier.

7 Project implementation

A result of this research is also to develop project instructions, that can be utilized for implementation of the water electrolysis plant project. Regardless of the power electronics supplier, selection of the rectifier affects power quality and reactive power, as shown by the theory and simulation results presented in this thesis. Understanding the origin of harmonics, power grid parameters and requirements for power quality and reactive power gives also requirements for design of the industrial power network. Project instructions made are based on the front-end loading (FEL), where the definitions are made in early phase of the project. The FEL stages and progress are presented in Figure 32.

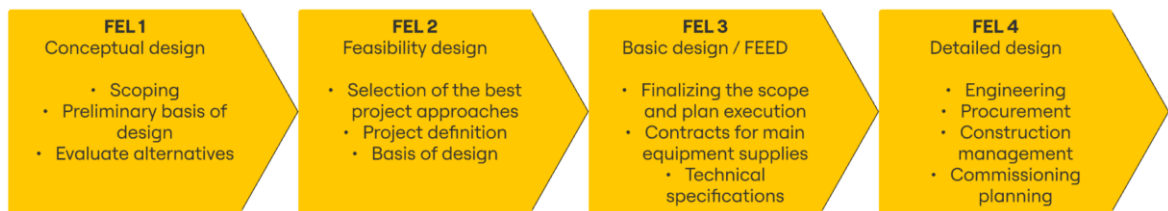


Figure 32. Simplified front-end loading process stages (EPCI Solutions, 2016).

The front-end loading defines design stages for the project implementation, where every stage has specified tasks. The FEL numbers are increasing according to the design level is progressing more detail. FEL 1 means conceptualization and FEL 4 is already the detailed design and execution, where for example procurement tasks are performed. (EPCI Solutions, 2016) These instructions focus on FEL levels 3 and 4, where process flow and detailed descriptions can be seen from Figure 33. Multiple different items and details affect project implementation and engineering, but this instruction is based on the requirements of power quality and reactive power related actions required in the project.

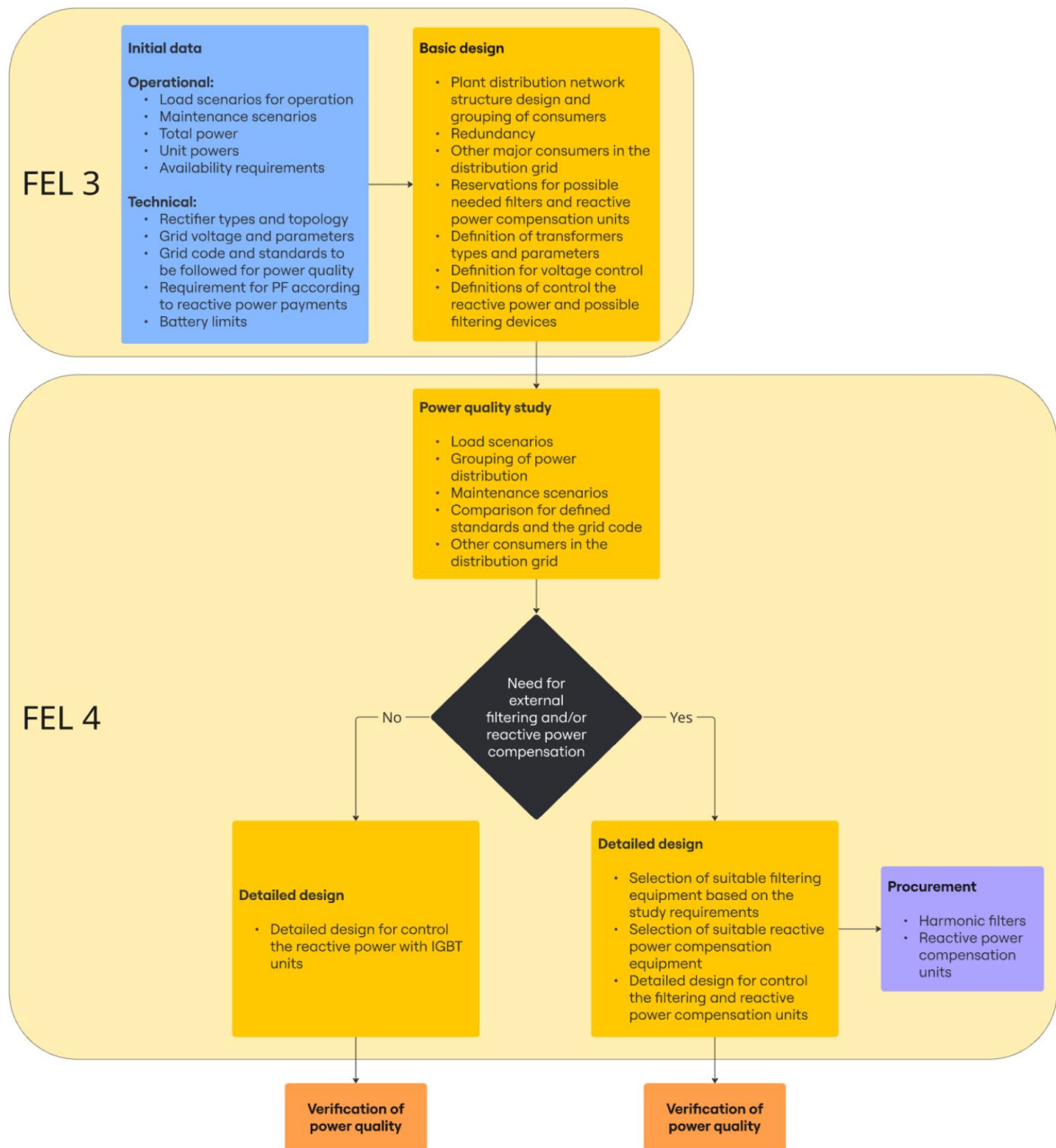


Figure 33. Process flow for project implementation.

The process flow diagram presents initial data, basic design work, study of harmonic distortion, detailed design with procurement and finally verification. Project phases what are out of the subject of this thesis are not included in the process flow diagram, like for example the installation phase. Descriptions of each project phases are opened in the next sub-titles.

7.1 Initial data for the project basic design work

Initial operational data is required for the basic design, where the plant total power and unit powers of the electrolyzers are needed. Part of the initial data will be created during the FEL3 implementation where other disciplines are working as well. Operational scenarios should be defined based on the hydrogen production needs, while also considering other requirements, such as operational mode recommendations from the electrolyser technology supplier. Cost optimization for the entire process should be investigated, taking into account items as the efficiency of electrolyzers considering the load profiles. Maintenance requirements must also be considered, such as how many units are maintained simultaneously and possible malfunction scenarios. Availability requirements of the plant may lead also redundancy of the power supply which needs to be considered in the project.

The main technical initial data for the project basic design is electrolyser unit powers, the total plant power, selected rectifier type and topology, data from power grid connection and standards to be utilized as requirement for the power quality. Demand for power factor is based on reactive power payments charged by the grid operator.

Selection of rectifiers is part of the initial data scope where the totality and battery limits between the parties may vary. Purchasers can have requirements for the rectification technology, but the strict requirements may also limit the possible technology suppliers, as many electrolyser supplies are based on package deliveries, where the rectifying equipment is included as part of the electrolyser product scope. Both evaluated rectifier technologies are suitable for electrolyser control, but according to the simulation results the thyristors-based technology requires external reactive power compensation and filtering of harmonic currents to comply with the IEEE 519-2022 standard and the grid code. If the external reactive power compensation and harmonic current filtering equipment cannot be used, then the selection shall be oriented to the IGBT technology. Since the power quality is noted to be within standard limits in all scenarios when using IGBT technology, the IGBT technology can be also a safer solution for the project implementation if all the operational initial data is not available during the basic design phase. The IGBT technology enables active control of reactive power by the converter itself, which can be also beneficial in cases if the power grid requires production of reactive power from the water electrolyser plant. The IGBT technology can be stated to be more adaptable rectifier technology for the project implementation,

when comparing to the thyristor technology. This is because IGBT technology doesn't need external devices for compensating the reactive power and filtering the harmonics, based on the simulation results. When using the 24-pulse thyristor technology, the minimum controlled power shall be taken into account when designing the load scenarios, if the rectifier topology is selected in a way that is proposed in this thesis, where two units need to be equally loaded.

Parameters of the power grid where the plant will be connected define initial data for the project, not only the voltage level but also the short circuit power at the grid's PCC, which shows stiffness of the grid. The standard IEEE 519-2022 is also referring to the ratio of short circuit current and the demand load current where a higher ratio allows us to use higher limit values in the standard.

The grid code and standards for power quality to be followed shall be selected for the basic design. Requirements from the power grid operator are absolute, but the power quality level of the industrial network can be determined by the owner, considering the interdependence. For example, scenarios 3 and 4 with the thyristor model simulations are not at an acceptable level according to the IEEE 519-2022 standard, but the scenarios fulfill the requirements of Fingrid's report. Also, the safety margin for possible simulations should be considered due to the possibility of errors in initial data and simulations.

Reactive power fees affect plant OPEX costs, where the pricing depends on the power grid operator. Limit for capitalization of expenses shall be determined and taken into account for the basic design, as a level of allowed reactive power consumption. Thyristor-based rectifiers are naturally at the inductive side, but the IGBT rectifier can also produce capacitive reactive power towards the power network according to control parameters.

Battery limits for the project define actions needed during the design process, where needed initial data within the deliveries shall be described for the delivery contracts. For example, if the electrolyser supplier is delivering also power electronics, the supplier should have the best knowledge and would be the best party to investigate harmonics produced by the rectifiers. On the other hand, the supplier requires initial data from the grid parameters to evaluate the harmonic levels at the point of delivery limit. Other consumers connected to the distribution network affect the power quality, as well as reactive power, so the totality shall be considered when defining the distribution grid. When the contractual battery limits might

vary and are limited to a certain point, the overall responsibility shall be shared for the party, who takes the responsibility to define the standards to be utilized in an industrial network, and to be responsible for fulfilling the requirements of the grid code considering the total plant.

7.2 Basic design

Content of basic design may vary depending on project implementation method. The content described in this section is based on a project implementation, where the initial data is affecting engineering related to the power quality and reactive power. Basic design contains basic levels of engineering, and for example circuit diagrams are not done during this engineering stage. The basic design results are mainly definitions and single line diagrams for power distribution, as well as procurement materials for long lead items depending on the project schedule.

Power division should be considered in the MV power grid design, where the total power, unit powers and the operational initial data will give requirements for power network engineering. In large setups, the power network might be necessary to be divided into groups because of possible current loading limitations, where also operational initial data can affect the layout. Increasing the medium voltage level allows also higher level of power transmission. Grouping the power distribution network can give flexibility for maintenance purposes and redundancy purposes, where possible filtering and compensation devices can be divided into same groups. When operational needs are defined, the power distribution layout should be considered as well to follow the operational requirements. Redundancy can mean interconnections in the distribution network, where the power supply can be ensured for needed consumers during the maintenance or malfunctions. Especially when the rectifying is made by thyristor converters and the actual needs for external filtering is not known yet, it's recommended to be prepared with reservations for feeders at the MV switchgear according to the layout and define the control of filtering.

Transformer types and parameters should be defined during the basic design because the types vary depending on the selected rectifier type and topology. The power division and grouping of power distribution networks might affect the transformer types and parameters as well.

Voltage control at industrial power distribution grid comprises the MV network voltage and low voltage for the rectifiers. It's recommended to equip the main transformer with an on-load tap changer, so that the medium voltage can be controlled in all power scenarios and keep the MV voltage at the required level, since the MV distribution grid is often serving other process equipment and building related equipment as well. Voltage control for the rectifier equipment is also important to define, because the voltage level needed for electrolyzers will be increased while the electrolyzers are aging. Voltage control for thyristor rectifying plays an important role for power quality and reactive power as well, because it's beneficial to operate at the smallest possible firing angle regardless the operational scenario. Installing the on-load tap changers for rectifier transformers as well would help to optimize the firing angle and minimize the needs for external filtering and reactive power compensation. Possible on-load tap changers for the rectifier transformers will increase CAPEX costs for the project, which are not considered in chapter 6.

The main transformers short circuit impedance level U_k may give optimization possibilities for the medium voltage distribution network, because the stiffness of the power grid affects the capability of resisting the interference and also affects the possibility of using higher limit values in the IEEE 519-2022 standard at the MV grid. Often the short circuit current withstand capacity of power components limits the possible decrease of the main transformers U_k value.

The thyristor-based converters require external reactive power compensation equipment, what should be defined as to be connected in the distribution network. Control of the compensation equipment shall be defined regardless of the type of compensation equipment, where current and voltage measurements shall be in the applicable location of the distribution network. Grouping power distribution will affect the control of reactive power and also the number of compensation units needed, and other consumers shall be taken into account. If the distribution network includes redundancy, then the control of reactive power equipment should be designed also considering the supply direction of the connected switchgear or group and possible interlockings might be evaluated. Control of the reactive power shall be defined also in case the IGBT rectifying technology is used. Even though the IGBT technology enables the power factor control internally in the equipment, the total network shall be considered like at thyristor case. Control of reactive power needs measurements and

control loops where the grouping of power distribution and other consumers shall be taken into account.

7.3 Detailed design

Detailed design is a project phase where detailed design actions are implemented and most of the purchases are also done during the detailed engineering (EPCI Solutions, 2016). All equipment data sheets become available during the procurement actions proceed, which leads also to clarification of procurement material for the reactive power compensation equipment, if the required power and equipment type cannot be already defined in earlier phase of the project. Detailed design phase freezes also the procurement materials for possible filtering purchase and equipment type. Control of filtering devices and reactive power compensation need to be engineered at the detailed design phase according to specifications made by basic design.

7.3.1 Power quality study

Study for harmonic distortion should be executed after the main consumers are defined for the project and the power distribution structure is defined according to the process needs. Operational scenarios should be defined also for the study and comparison against the selected standards and grid code should be resulted. Possible grouping of distribution networks shall be modeled also in the study, where exceptional operational cases, such as for example malfunctions, are considered. The level of study shall be determined related to the power grid structure, utilized technology and according to available initial data. For example, it's not appropriate to simulate the rectifier operation itself, if the electrolyser supplier is providing harmonics data from the rectifying equipment already. Also, the exact information about the rectification equipment might not be available due to manufacturers' desire to protect the information. Collecting the information of rectifiers harmonic distortion, as well as the data from other consumers and considering this as a totality according to the operational scenarios and comparing the results for the selected standards and grid code should be the integrators' role. If the initial data is not available from equipment suppliers, the review should go to the device level and take the devices themselves into account in more detail, with the precision

that is possible. If the major deviations are found during the study, the findings might cause also a need to change the specifications made in the basic design. The study should be done in the project even though the IGBT technology is selected, because variations might occur between the manufacturers and other consumers might also cause unexpected harmonic distortion. The main result of the power quality study is the decision of needed external filtering and reactive power compensation devices with the required performance, which can be utilized directly in the request of quotation.

7.4 Verification of power quality and reactive power

It's recommended to verify the power quality at operational scenarios defined during the hot commissioning phase. Verification of the power quality can be made by using an analyzing service or installing needed fixed instruments into switchgears where the harmonic content and reactive power can be followed on-line. Possible fixed measurement instruments shall be specified for the procurement of switchgears.

8 Conclusions

The research achieved the objectives defined and knowledge increased for requirements of design the large-scale water electrolysis plant considering the power quality and reactive power. Theory of single rectifier unit is important to understand, but when operating the large-scale hydrogen production, the operational methods and scenarios affect the totality built by multiple rectifying units, where the modelling gave new perspective about the behaviour of harmonics. Since the water electrolyser plant processes are relatively energy-intensive and the industry sector is growing, influence of the power quality will be also in a higher role in the future.

8.1 Key findings

When the grid code is definitive to follow and standards are recommendations, the selection of utilized standard shall be considered for the project basic design as initial data. Power quality at the 110 kV PCC is dependent of the power quality in the plant distribution grid, but according to the simulation results, part of the scenarios achieves the Fingrid requirements even the power quality doesn't comply with the IEEE 519-2022 recommendations. Based on the simulation results, we can also summarize that fulfilling the IEEE 519-2022 recommendations gains also the requirements of Fingrid and is therefore a safe selection for applicable standard. Different standards are having different point of views, and it makes challenging to define the limit values to follow. For example, IEEE 519-2022 refers to the maximum demand load current, which can be challenging to define for the green-field project. This makes important to define the load profiles of the hydrogen plant in early phase.

Importance of operational scenarios on the partial loads is one of the key findings in this thesis. Definitions of operational scenarios can lead decisions in the detail level, what needs to be considered already at the basic design phase of the project. Maintenance activities for the future should be notified as operational scenarios, because that can also affect the design of the power distribution grid.

The thyristor-based rectifiers have better characteristics of harmonic distortion with the higher the pulse count is chosen for the topology. However, when operating the 24-pulse

units, it should be noted that according to the Fourier series, the 24 ± 1 harmonic magnitude are summed and because of these currents, it's challenging to reach the limits of the applicable standards, even the total harmonic distortion and total demand distortion values are at an acceptable level. These observed harmonic currents cause the need to use the external filtering based on the simulation models. Controlling of the thyristor rectifiers is done by changing the firing delay angle, but the higher firing angle value is affecting also the higher reactive power and harmonic distortion. Based on this observation, voltage control of the grid comes more important when using the thyristor-based rectifiers to optimize the firing delay angle and thus minimize the reactive power and harmonic distortion. External reactive power compensation is also required to avoid the reactive power payments charged by the grid operator when utilizing the setup defined for the simulation.

The IGBT is an active bridge rectifier that has limitations of withstanding high currents and that's why the topology comes more complex, which leads more parallel units in the topology. Controlling of force commutated rectifier requires also more complex control loops, but benefits are realized with capability to control the reactive power by the converter itself, and no external compensation units are needed. The IGBT topology simulated performs better in providing the harmonic distortion and fulfils all standard limits reviewed in this research. The IGBT technology can be kept more adaptable solution in cases, where all initial data is not available for the basic design, considering the operational scenarios.

THDi values of the converters can be utilized as comparison between technologies, but according to the simulation results the THDi or TDDi values are not the reasons why limits of the applicable standards are not reached. Crossing of the standard limits occurs with single frequencies, which are not so high, that for example the total demand distortion would be out of the standard limitation. This should be noted especially when considering the thyristor-based technology.

CAPEX costs division differs between technologies for the rectifier equipment and the rectifier transformers. The IGBT based equipment are more expensive itself, but because the thyristor-based technology requires special transformers and external reactive power compensation units, the total price difference between the technologies is in 5%, where the thyristor-based technology appears lower in CAPEX costs. However, based on the simulation results, the thyristor-based technology requires also external filtering against the harmonic distortion, what is not concluded in the CAPEX comparison. Possibility to use an active

filtering solutions, where the same equipment can compensate the reactive power should be investigated.

Selection of the rectifier technology can be based on for electrolyser technology suppliers' choice, and that's why it's important to understand the requirements of the distribution grid from engineering point of view. Instructions for project implementation concludes steps for the basic design items and correct timing of initial data available to ensure the smooth project flow and avoiding surprises during the project implementation. Study for harmonic distortion proposed in the detailed design phase is important step of the project and initial data from the power electronics supplier is a vital for success. Simulink model might be difficult to utilize considering other consumers as well in the distribution grid and the needed data available from the power electronic suppliers. The other modelling solutions are recommended to investigate based on the data supplied by manufacturers and conclude the totality. The role of the integrator cannot be overemphasized in a situation where a complex hydrogen plant consists of electrical drives and electrification solutions from several different suppliers.

8.2 Recommendations for the future studies

Applying standards can be challenging due the different conditions between the standards. Practical instructions of utilizing the standards related to power quality and possible harmonization would help the future projects since the markets of water electrolyser systems is growing.

Simulation is used as research method and experiences of the simulation results for development actions. Importance of voltage control for the thyristor model was observed in the simulation results, where the results of better optimization implementation could be investigated. Implementing the on-load tap changer for rectifier transformers would help to optimize the voltage and reduce harmonic distortion and reactive power. Modelling the electrolyser itself would also give better controllability of the system and realistic DC characteristics would give results for impact of electrolyser parameters to the power quality.

This research focuses only on power quality and reactive power, but energy efficiency and lifecycle cost are also relevant items, that influence the selection of technology. Energy

efficiency with possible heat recovery possibilities and differences for lifecycle costs would be investigated in separated research.

8.3 Final words

The entire process, which includes understanding the theory, applying standards, basis of design, equipment selection, design tasks and cost optimization, forms a totality, what is vital for the success in projects. Electrical power distribution plays a key role in energy-intensive processes, where this research focuses on power quality and reactive power management and supports the future green hydrogen projects.

References

- ABB. 2000. ABB:n tekninen käsikirja 2000-7, 7. Oikosulkusuojaus. 20 pages. Available: https://heikkilaakso.com/opetus/abb/071_0007.pdf
- ABB. 2017. Technical guide No. 6, Guide to harmonics with AC drives. 32 pages. Available: https://library.e.abb.com/public/bc35ffb4386c4c039e3a8ec20cef89c5/Technical_guide_No_6_3AFE64292714_RevF_EN.pdf
- EPCI Solutions. 2016. Front End Loading. Web page. Available: <https://www.georgeralston.com/front-end-loading.html>
- Fingrid. 2015. Power quality in Fingrid's 110 kV grid. Available: https://www.fingrid.fi/globalassets/dokumentit/en/customers/grid-connection/20150911_110-kv_verkon_sahkonlaatu_en.pdf
- Giroux, P., Sybille, G., Hydro-Quebec (IREQ). 2024. AC/DC Three-Level PWM Converter, Simulink 2022b documentation
- Guo, X. Zhu, H. Zhang, S. 2023. Overview of electrolyzer and hydrogen production power supply from industrial perspective. International Journal of Hydrogen Energy. Vol. 49. p. 1048-1059.
- Hassan,Q. Algburi, S. Jaszczur, M. Al-Jiboory, A. Musawi, T. Ali, B. Viktor, P. Fodor, M. Ahsan, M. Salman, H. Sameen, A. 2024. Hydrogen role in energy transition: A comparative Review. Process Safety and Environmental Protection. Vol. 184. p. 1069-1093.
- Heikkinen, M. 2024. Personal communication. Unpublished.
- Helen Oy. 2025a. About us, Helen. Web page. Available: <https://www.helen.fi/en/about-us/helen/about-helen>
- Helen Oy. 2025b. About us, Hydrogen. Web page. Available: <https://www.helen.fi/en/about-us/energy/hydrogen>
- Helen Sähköverkko. 2021. Price list for electricity network services for 110 kV. Available: https://www.helensahkoverkko.fi/globalassets/hinnastot-ja-sopimusehdot/hsv---enkku/price-list-for-electricity-network-services-for-110kv_en.pdf

Helen Sähköverkko. 2025. Sähköliittymien hinnasto. Available: https://www.helensahko-verkko.fi/globalassets/hsv/hsv-pdf/ohjeet/sahkoliittymat_20250101_1.pdf

IEEE 519-2022. IEEE Standard for harmonic control in electric power systems. New York: The Institute of electrical and electronics engineering. 31 pages.

Jakobsen, R. Huang, C. Rasmussen, T. You, S. 2022. Large-scale electrolyzer plant integration to the electrical grid: Preliminary investigation of VSC-based solutions. 7th International Conference on Renewable Energy and Conservation, November 18-20, Paris, France.

Keddar, M. Zhang, Z. Periasamy, C. Doumbia, M. 2022. Power quality improvement for 20 MW PEM water electrolysis system. International Journal of Hydrogen Energy. Vol. 47. p. 40184-40195.

Koponen, J. Poluektov, A. Ruuskanen, V. Kosonen, A. Niemelä, M. Ahola, J. 2021. Comparison of thyristor and insulated-gate bipolar transistor -based power supply topologies in industrial water electrolysis applications. Journal of Power Sources. Vol. 491. 229443.

Liao, J., Yeh, S. 2000. A Novel Instantaneous Power Control Strategy and Analytic Model for Integrated Rectifier/Inverter Systems. IEE Transactions on power electronics. Vol. 15. No. 6. P.996-1006.

MathWorks. 2024a. Pulse Generator (Thyristor). Documentation for Simulink Pulse Generator block. Available: <https://se.mathworks.com/help/sps/powersys/ref/pulsegenerator-thyristor.html>

MathWorks. 2024b. Park Transform. Documentation for Park Transform block. Available: <https://se.mathworks.com/help/sps/ref/parktransform.html>

McGraw, M. 2025. An 'Intuitive Understanding' of Electrical Harmonics: A conversation. Available: <https://www.mirusinternational.com/downloads/Intuitive%20Understanding%20of%20Harmonics%20210624.pdf>

McKinsey & Company, Hydrogen Council. 2024. Hydrogen Insights September 2024. Available: <https://hydrogencouncil.com/wp-content/uploads/2024/09/Hydrogen-Insights-2024.pdf>

Mohammed, S. Teh, J. Kamarol, M. 2019. Power Quality Improvements in a Novel 24-Pulse Line Commutated Converter HVDC Transmission System. 10th International Conference on Robotics, Vision, Signal Processing and Power Applications. Lecture Notes in Electrical Engineering. Vol. 547. Springer, Signapore. p. 221-227.

Mohan, N. Undeland, T. Robbins, W. 2003. Power Electronics. Converters, Applications and Design. Third Edition. John Wiley & Sons, Inc.

Nafchi, F. Afshari, E. Baniyadi, E. Javani, N. 2019. A parametric study of polymer membrane electrolyser performance, energy and exergy analyses. International journal of hydrogen energy. Vol. 44. p.18662-18670.

Nerg, J. 2024. Personal communication. Unpublished

Orkola, P. 2024. Helenin vetylaitos tuo markkinoille uudenlaista joustavuutta. Blog post. Available: <https://www.helen.fi/blogi/2024/helenin-vetylaitos-tuo-markkinoille-uudenlaista-joustavuutta>

Peltoniemi, P. 2024. Personal communication. Unpublished

Rashid, M. 2011. Power electronics handbook. Devices, circuits and applications. Third edition. Butterworth-Heinemann.

SFS-EN 50160:2022. Voltage characteristics of electricity supplied by public electricity networks. Helsinki: Finnish Standards Association SFS. 107 pages.

Appendix 1. Psophometric weighting factors (Fingrid, 2015)

h	P _h	h	P _h	h	P _h	h	P _h	h	P _h
1	0.7	21	1109	41	698	61	513	81	161.3
2	8.9	22	1072	42	689	62	501	82	144.5
3	35.5	23	1035	43	679	63	487	83	130.3
4	89.1	24	1000	44	670	64	473	84	116
5	178	25	977	45	661	65	458.5	85	104.2
6	295	26	955	46	652	66	444	86	92.3
7	376	27	923	47	643	67	428	87	82.4
8	484	28	905	48	634	68	412	88	72.4
9	580	29	881	49	625	69	394	89	64.3
10	661	30	861	50	617	70	376	90	56.2
11	733	31	842	51	607	71	355.5	91	50
12	794	32	824	52	598	72	335	92	43.7
13	851	33	807	53	590	73	313.5	93	38.8
14	902	34	791	54	580	74	292	94	33.9
15	955	35	775	55	571	75	271.5	95	30.1
16	1000	36	760	56	562	76	251	96	26.3
17	1035	37	745	57	553	77	232.5	97	23.4
18	1072	38	732	58	543	78	214	98	20.4
19	1109	39	720	59	534	79	196	99	18.2
20	1122	40	708	60	525	80	178	100	15.9

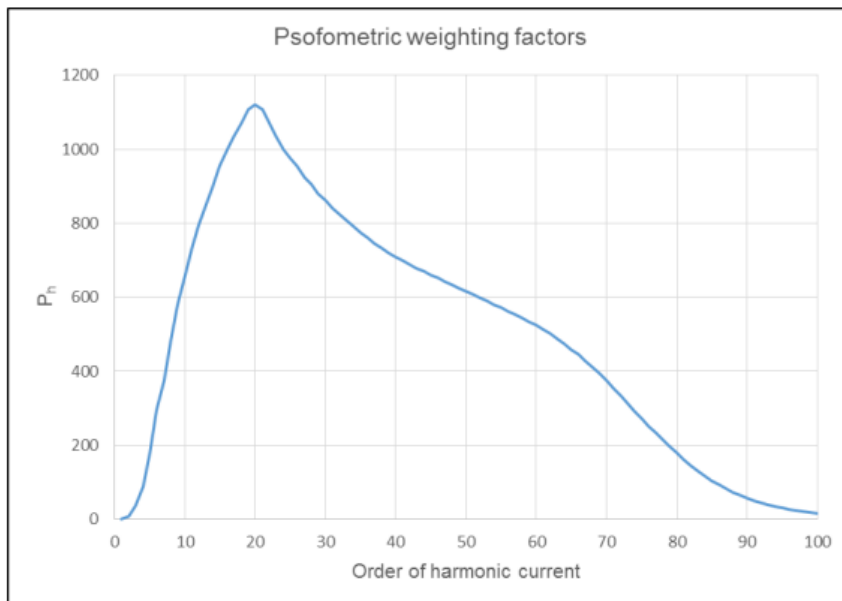


Figure 1. Psophometric weighting factors at different harmonics. The exact values are given in the table.

Appendix 2. Scenario 1: Current and voltage waveforms of thyristor model

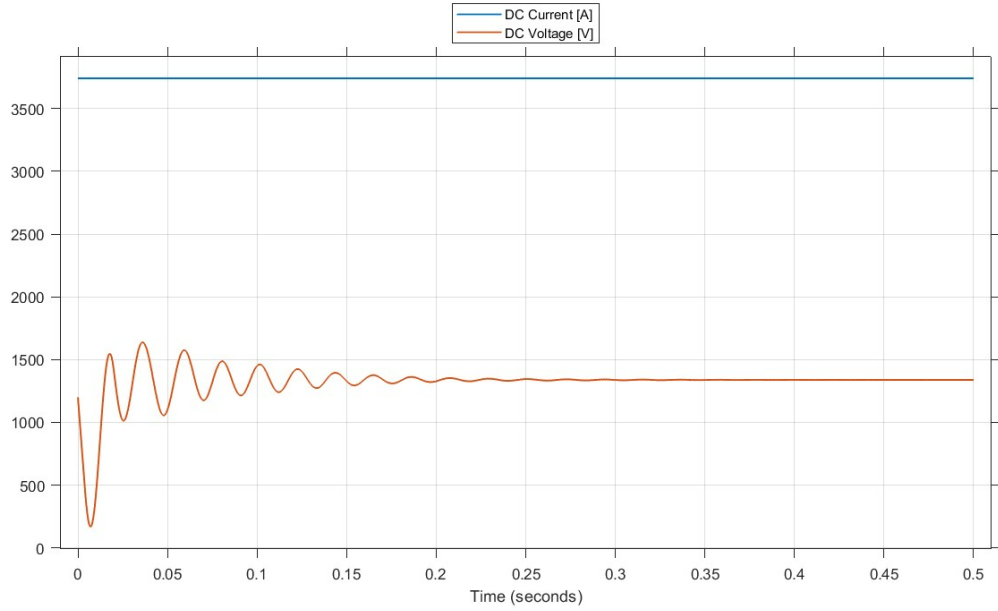


Figure 1. DC voltage and current of single electrolyser, 100% load.

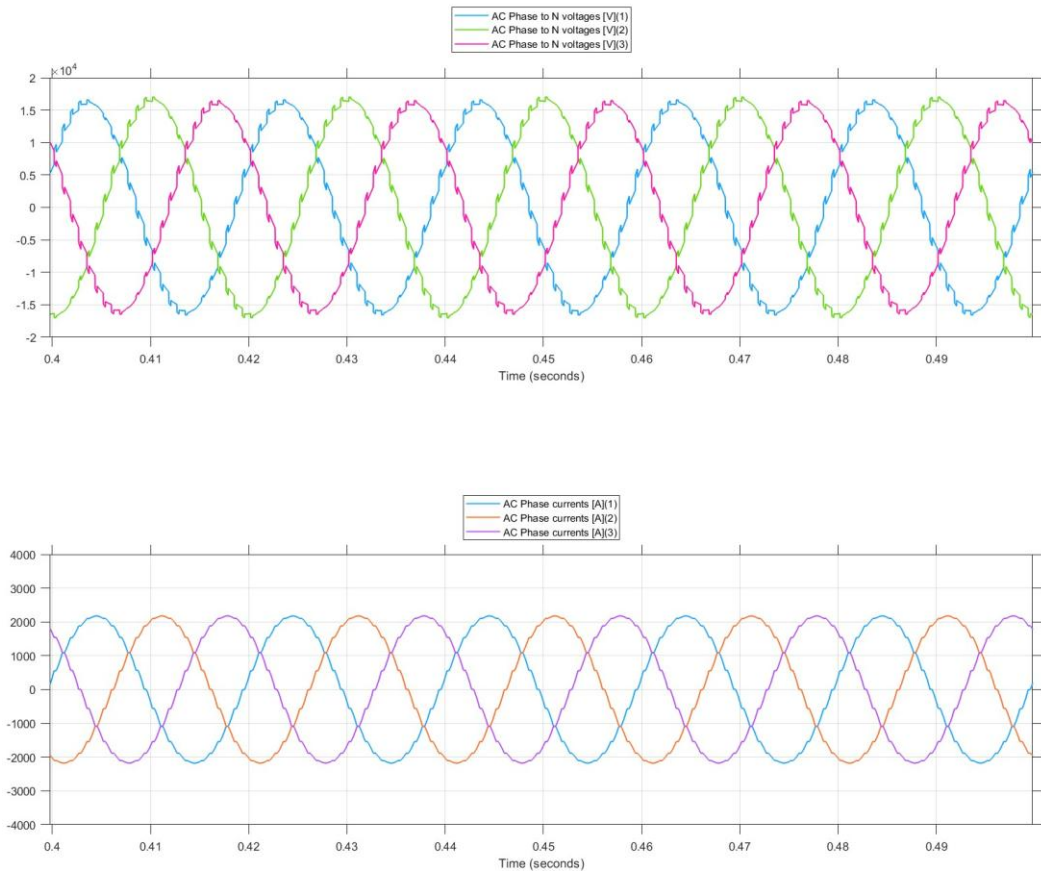


Figure 2. AC voltages and currents at 20 kV voltage step, 100% load.

Appendix 3. Scenario 3: Current and voltage waveforms of thyristor model

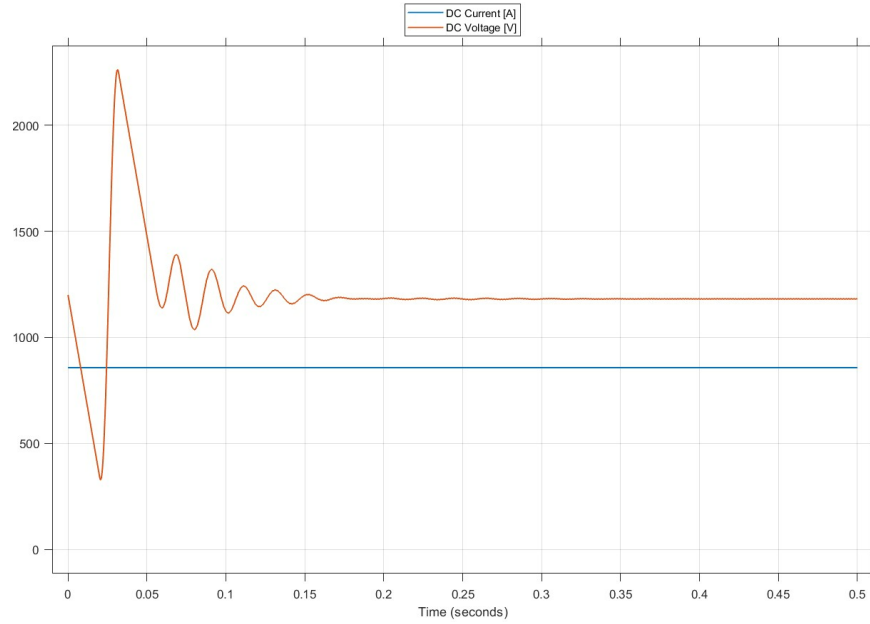


Figure 1. DC voltage and current of single electrolyser, 20% load.

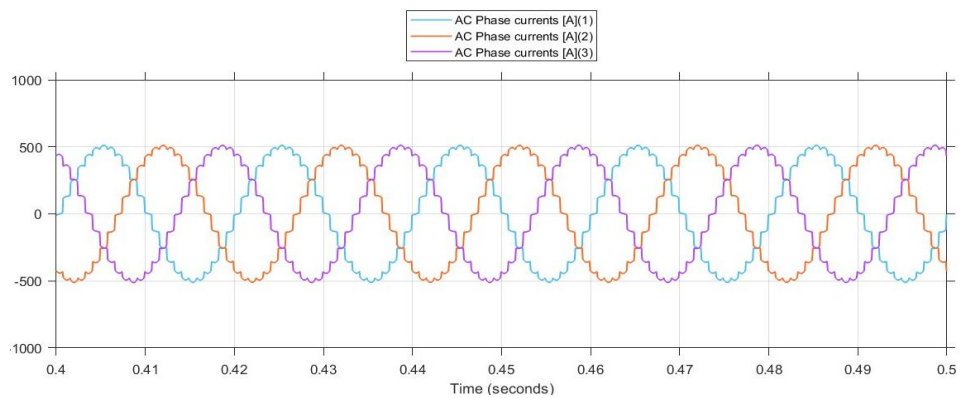
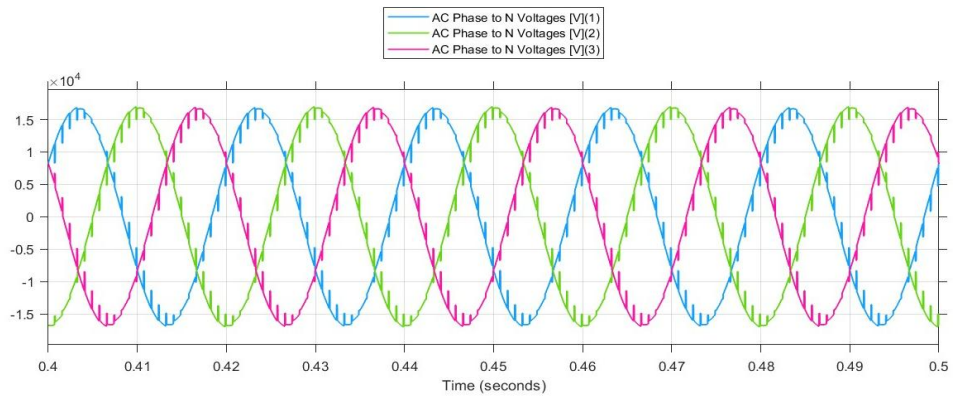


Figure 2. AC voltages and currents at 20 kV voltage step, 20% load.

Appendix 4. Scenario 1: Current and voltage waveforms of IGBT model

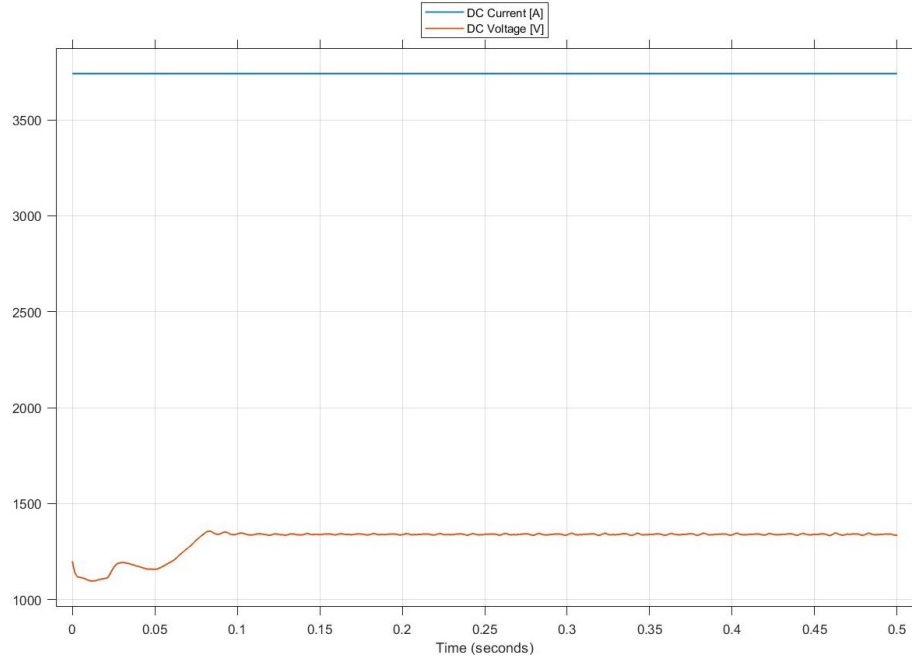


Figure 1. DC voltage and current of single electrolyser, 100% load.

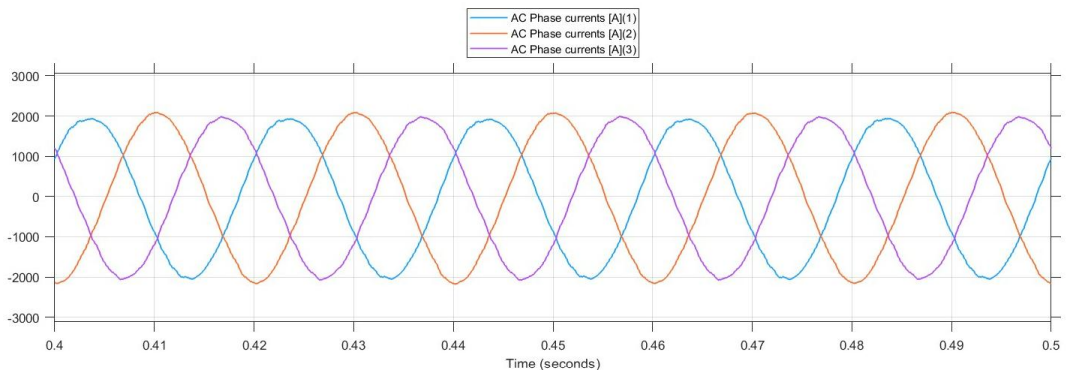
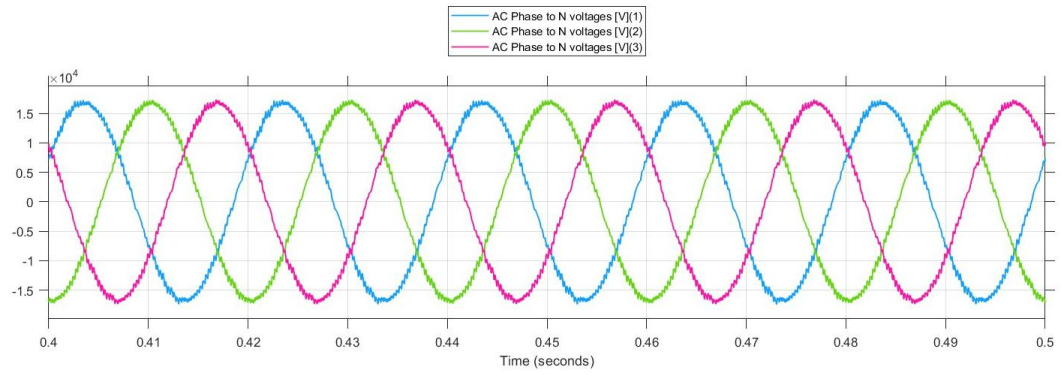


Figure 2. AC voltages and currents at 20 kV voltage step, 100% load.

Appendix 5. Scenario 3: Current and voltage waveforms of IGBT model

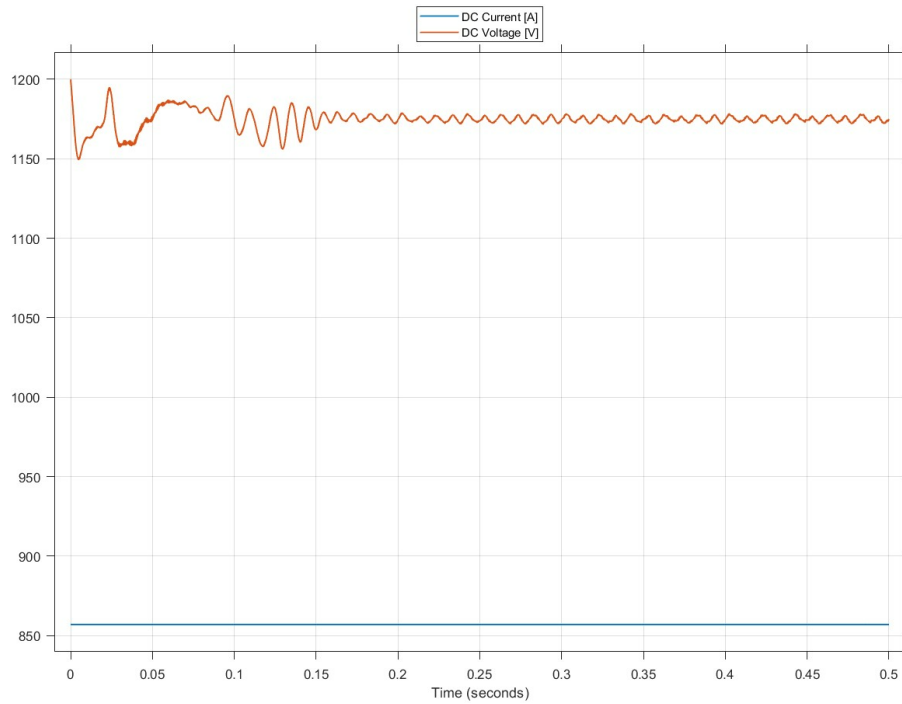


Figure 1. DC voltage and current of single electrolyser, 20% load.

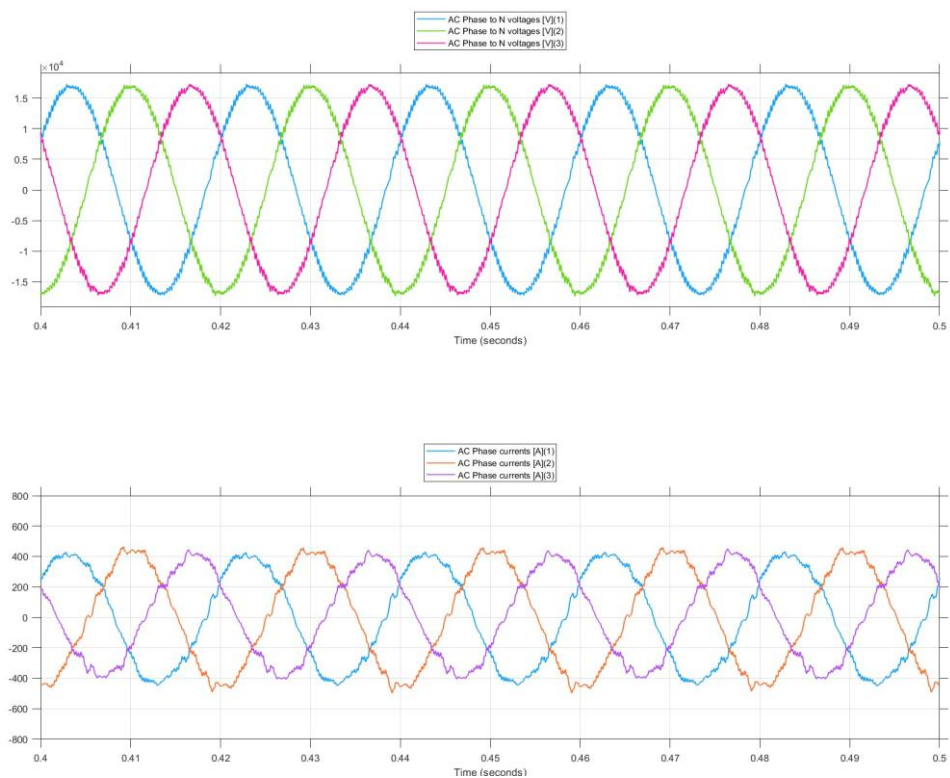


Figure 2. AC voltages and currents at 20 kV voltage step, 20% load.